SUPPLEMENTARY INFORMATION

Raj et al.

METHODS

Cell death assays. Apoptotic cell populations were determined by TUNEL assay (Roche, IN). Cells were grown in 6-well pates or 100mm petri-dishes were trypsinized, recovered by centrifugation at 300 x g, and fixed in 2 % paraformaldehyde-PBS for 16 hours. Cells were then washed twice with PBS and re-suspended in fresh permeabilization solution (0.1% Triton-X 100 and 0.1% Sodium citrate) for 30 minutes at room temperature. Enzymatic labeling of free 3'-OH DNA ends with dUTP-conjugated to TMR red was performed according to the manufacturer's protocol. The percentage of TUNEL positive apoptotic cells was determined by flow cytometry enumeration of fluorescent cells (FL2-H: 570 - 620 nm). Cell viability was also determined by crystal violet staining (0.2% w/v in 2% ethanol), Trypan blue exclusion (Invitrogen, CA) and Alamar-blue cell viability assay (Invitrogen, CA). For Trypan-Blue exclusion assay, equal number of cells for each cell line ($1x10^5$) were plated in 6-, 12- or 24-well plates and allowed to reach 60-70% confluency. The cells were then treated with different concentrations of PL and incubated for the appropriate time points. The cells were then trypsinzed and stained with trypan Blue and the viable and dead cells counted using a hematocytometer. For every sample a total of 300 cells were counted in triplicates and the percentage of non-viable cells were plotted graphically with standard deviation. For Crystal violet Staining, cells were plated in 6 -well and 12- well plates. Having reached confluency of 60-70%, the cells were then treated with PL for 12 and 24 hours. Following the treatment time the medium was removed; cells were then washed in PBS and fixed in 3.7%

formaldehyde for 15 minutes before staining with Crystal violet stain for visual quantification of cell viability. For Alamar blue cell viability assay, cells were plated and treated in 48- or 96-well plates, after which 10% of Alamar blue was added and incubated at 37°C for an additional 2 hours. Fluorescence was measured (excitation/emission: 530/590) on a VictorX3 plate reader and the cell viability was calculated by plotting fluorescence emission intensity versus compound concentration and treatment time (a reduction in Alamar blue fluorescence correlates to decrease in cell viability).

Animal experiments: All animal experiments were reviewed and approved by the Massachusetts General Hospital Subcommittee on Research Animal Care.

Assaying of total cellular glutathione. Cells were treated with PL and NAC for the appropriate time points. A total number of $1x10^6$ cells were collected into 1.5 ml centrifuge tubes and centrifuged at 700 x g for 5 minutes and the cell pellets were lysed in 100ul of ice-cold lysis buffer. After incubating on ice for 10 minutes, the lysate was centrifuged for 10 minutes and the supernatant was used for glutathione assay following the manufactures instruction for ApoGSH glutathione detection kit (BioVision Research Products, Mountain view, CA). The total amount of GSH was measured using a fluorescence plate reader at Ex./Em. = 380/460nm.

Quantification of glutathione disulfide (GSSG). Tumor and normal cells were treated with PL for the appropriate time points. Quantification of GSSG was essentially performed using the manufactures instructions for a microplate assay for GSH/GSSG (Oxford Biomedical Rsearch, Inc, Oxford, MI). A total number of

$0.5x10^6$ cells were collected in 1.5 ml centrifuge tubes containing ice-cold buffer with the thiol scavanger to keep GSSG in its oxidized form. The cells were homogenized with a Teflon pestle and the cell suspension sonicated in icy water for 2-3 minutes. Ice-cold metaphosphoric acid was added to deproteinate the samples. The samples were centrifuged at 1000 x g at 4°C and the supernatants were used for determining the GSSG concentration according to the manufactures protocol using a microplate reader with 405 nm filter. The change in GSSG levels in PL treated samples was expressed as fold change compared to control (DMSO) treated samples.

Measurement of GSTpi enzymatic activity. The GSTpi-specific activity was measured by using ethacrynic acid, a GSTpi class–specific substrate. For each assay 200 μg of cellular proteins was used in a final reaction volume of 200 μl that contained 100 mM potassium phosphate buffer (pH 6.5), 1 mM EDTA (pH 6.5), 0.25 mM glutathione and 0.2 mM ethacrynic acid. The amount of ethacrynate-GSH conjugates was measured by spectrophotometry with the Nanodrop ND-1000 (Nanodrop Technologies, Inc.) at 270 nm. The GSTpi enzymatic activity of the DMSO treated sample was arbitrarily was defined as 100% and the change in GSTpi activity in PL treated samples was plotted accordingly. In the assay for in vitro measurement of GSTpi enzymatic activity, recombinant GSTpi protein (PROSPEC, Inc.) was used instead of total cellular protein extract and GSTpi activity was performed as mentioned above.

Measurement of ROS production. Cells were treated with PL, DMSO or paclitaxel for 1 and 3 hours and ROS generation was detected with 2'-, 7'-

dichlorofluorescein diacetate (DCFH-DA) (Invitrogen, Carlsbad, CA, USA). Cells were incubated with 10 μM of DCFH-DA for 30 min at 37°C, washed twice with PBS and immediately analyzed by a FACScan flow cytometer. The antioxidant NAC (N-acetly-L-cysteine) was used at 3mM concentration. Histograms are representative of three separate experiments.

Measurement of cellular superoxide anion level. Hydroethidine (Invitrogen, Carlsbad, CA, USA) was used to detect cellular superoxide levels in various cell lines, including EJ and U2OS cells, and normal cells after 2 hours of treatment with PL. The cells were labeled with 10 μM of Hydroethidine (Het) for 60 min and superoxide was measured by a FACScan flow cytometer. Histograms are representative of three separate experiments.

Measurement of nitric oxide production. Cells were treated with PL for 1 and 3 hours and nitric oxide generation was detected with 4-amino-5-methylamino-2'-, 7'-difluofluorescein diacetate (DAF-FM diacetate) (Invitrogen, Carlsbad, CA, USA). The cells were labeled with 3μM of DAF-FM diacetate for 60 minutes at 37°C. Following staining cells were washed with fresh media and incubated for with fresh media for an additional 15 minutes at 37°C to allow for complete de-esterification of the intracellular diacatates. Then cells were trypsinized and the nitric oxide (NO) radical measured by a FACScan flow cytometer. Histograms are representative of three separate experiments.

Measurement of mitochondrial membrane integrity. The mitochondrial membrane potential of PL-treated and untreated cells was assayed by using rhodamine-123 (Invitrogen, Carlsbad, CA, USA). Cells were treated with PL for 0,

9, 18 and 24 hours and stained with 1 μM of rhodamine-123 for one hour at 37°C. Following the staining, the cell was washed with PBS twice and harvested for FACScan analysis.

Cytochrome c release. Induction of cytochrome c release from mitochondria to cytosol by PL was measured by cell fractionation followed by western blotting. Mitochondria and cytosolic fractions were separated by differential centrifugation. Release of cytochrome c to the cytosol in cytosol fraction was detected by western blot analysis using a Cyt-c antibody (Invitrogen). β-actin was used as the loading control for cytosolic extracts.

Comet Assay. Cells were treated with PL and ETO for 18-24 hours and processed for comet assay following manufactures instruction (TREVIGEN, Gaithersburg, MD, USA). Briefly, $1X10^5$ cells were resuspended in 1 ml of cold PBS and 30 μl of the suspension was mixed with 300 μl of molten agarose. The agarose-embedded samples was spread on to the comet slides and allowed to set at 4°C for 30 minutes. The comet slides were immersed in the lysis solution and incubated over-night at 4°C. Following lysis, the slides were immersed in freshly prepared alkaline buffer for 60 minutes in dark. The slides were then rinsed in 1XTBE, electrophoresis was conducted at a set voltage of 1 Volt /cm for 20 minutes, dehydrated in 70% ethanol and air-dried in dark. The dried slides were stained using DNA-bound SYBER Green I fluorescence stain. For visualization of DNA damage images were captured using a 63X objective on a Leica TCS-NT confocal microscope.

Preparation of Affinity Matrices.

Reagents. L-arginine-13C6 and L-lysine-13C615N2 were from Sigma Isotec (St. Louis, MO). The cell culture media, Dulbecco's Modified Eagle's Medium (DMEM) deficient in arginine, lysine and methioine, was a custom media preparation from Caisson laboratories (North Logan, UT). All other L-amino acids were obtained from Sigma. Dialyzed serum was obtained from SAFC-Sigma. Trypsin was from Promega (Madison, WI) and U2OS and EJ were from ATCC (Manassas, VA).

Preparation of piperlongumine analogs and general procedure of solid-phase immobilization. All chemicals were purchased from Sigma-Aldrich and common solvents were purchased from Fisher (J.T.Baker) at HPLC grade unless otherwise noted. Piperlongmine **(1)** was purchased from Indofine Chemical Company (Catalog #: P-004, 97%, Hillsborough, NJ). Automated flash chromatography was performed on Teledyne ISCO CombiFlash Rf systems. LC and mass spectra were collected on either a WATERS Micromass ZQ or a WATERS Alliance 3100 system. ^{1}H and ^{13}C-NMR spectra were collected on a Bruker 300 MHz. NMR spectrometer. All HRMS were collected on a Bruker Daltonics APEXIV 4.7 FT-ICR Mass Spectrometer.

Abbreviations:

DCM: dichloromethane

DEAD: diethyl azodicarboxylate

DMF: *N,N'*-dimethylforamide

DMSO: dimethyl sulfoxide

EDC: 1-ethyl-3-(3-dimethyllaminopropyl)carbodiimide hydrochloride

NHS: *N*-hydroxysuccinimide

PBS: phosphate buffered saline

TEA: triethylamine

TFA: trifluoroacetic acid

THF: tetrahydrofuran

TPP: triphenylphosphine

(E)-3-(3,4,5-trimethoxyphenyl)acryloyl chloride (3)

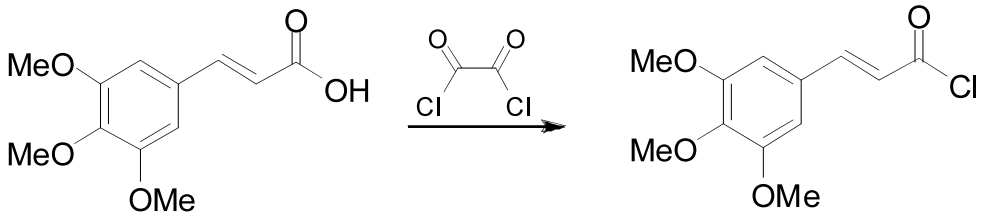

394.5 mg of starting acid (E)-3-(3,4,5-trimethoxyphenyl)acrylic acid **(2)** (1.656 mmol) was dissolved in 564 µL (3.89 eq.) of Oxalyl Chloride in a flame-dried flask at 0 ºC. The reaction was stirred while being slowly warmed to room temperature for 1 hour. The reaction mixture was dried over vacuum and to afford the product (E)-3-(3,4,5-trimethoxyphenyl)acryloyl chloride **(3)** directly as a yellow solid. (422 mg, 99%). The product was used for the next step without further purification.

(E)-1-(3-(3,4,5-trimethoxyphenyl)acryloyl)piperidin-2-one (4)

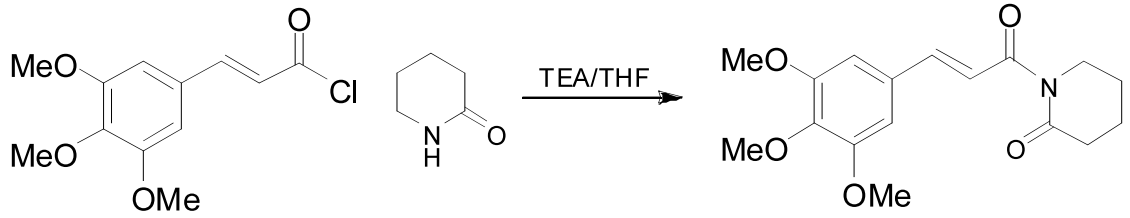

185 mg of ((E)-3-(3,4,5-trimethoxyphenyl)acryloyl chloride **(3)** (0.721 mmol, 1.1 eq.) was dissolved in 1 mL anhydrous THF at 0 ºC and 183 µL of anhydrous TEA (1.311 mmol, 2.0 eq.) was added to the solution. The mixture was stirred for 15 min then 65.0 mg piperidin-2-one (0.656 mmol, 1.0 eq.) in 5.0 mL anhydrous THF was slowly added under nitrogen. The mixture was stirred at room temperature overnight. The reaction mixture was then diluted with 10.0 mL DCM, washed with saturated NH_4Cl and brine, concentrated and then purified by flash chromatography. The product was obtained as a white solid. (183.7 mg, 89%) 1H NMR (300 MHz, CDCl3) δ 7.61 (d, 1H, J = 15.6), 7.33 (d, 1H, J = 15.5), 6.77 (s, 2H), 3.86 (d, 9H, J = 4.3), 3.77 (s, 2H), 2.58 (s, 2H), 1.85 (m, 4H). 13C NMR (300 MHz, CDCl3) 173.86, 169.53, 153.32, 143.33, 139.91, 130.67, 121.34, 105.40, 60.92, 56.15, 44.60, 34.93, 22.55, 20.61. HRMS (ESI/FT-MS): 320.1490$[M+H]^+$; expected 320.1492.

(E)-1-(3-(3,4,5-trimethoxyphenyl)acryloyl)pyridin-2(1H)-one (5)

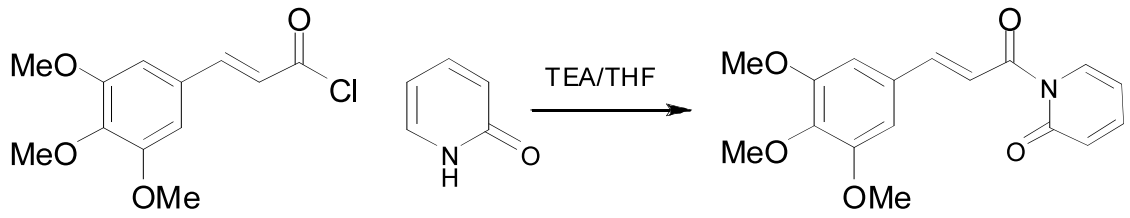

193 mg of (E)-3-(3,4,5-trimethoxyphenyl)acryloyl chloride **(3)** (0.752 mmol, 1.1 eq.) was dissolved in 1 mL anhydrous THF at 0 ºC and 191 µL of anhydrous TEA (1.367 mmol, 2.0 eq.) was added to the solution. The mixture was stirred for 15 min then 65.0 mg pyridin-2(1H)-one (0.683 mmol, 1.0 eq.) in 5.0 mL anhydrous THF was slowly added under nitrogen. The mixture was stirred at room temperature overnight. The reaction mixture was then diluted with 10.0 mL DCM, washed with saturated NH_4Cl and brine, concentrated and then purified by flash chromatography. The product was obtained as a white solid. (150.6 mg, 69.9%). 1H NMR (300 MHz, CDCl3) δ 8.39 (dd, 1H, J = 1.6, 4.6), 7.76 (ddd, 2H, J = 9.9, 11.9, 21.5), 7.19 (ddd, 2H, J = 14.4, 19.0, 19.8), 6.75 (s, 2H), 6.46 (dd, 1H, J = 15.8, 35.9), 3.84 (d, 9H, J = 4.4). 13C NMR (300 MHz, CDCl3) 164.74, 158.03, 153.45, 148.57, 147.24, 140.54, 139.45, 129.49, 121.98, 116.48, 116.03, 105.56, 60.93, 56.13. HRMS (ESI/FT-MS): 316.1187 $[M+H]^+$; expected 316.1179.

(E)-1-(3-(4-hydroxy-3,5-dimethoxyphenyl)acryloyl)-5,6-dihydropyridin-2(1H)-one (6)

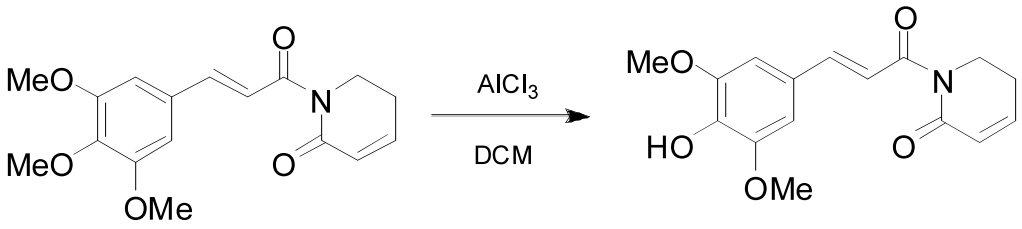

950 mg (2.99 mmol, 1.0 eq.) Piperlongumine **(1)** was dissolved in a flame-dried flask by 10.0 mL of anhydrous DCM. At room temperature, 2.834 g $AlCl_3$ (21.26 mmol, 7.1 eq.) was added to the solution. $AlCl_3$ cannot be completely dissolved in the solution and the yellow suspension formed was stirred at room

temperature for 1 hour. The reaction mixture was diluted with DCM, washed with saturated NH_4Cl and water. The organic phase was dried over Na_2SO4 and the product was isolated by flash chromatography. (800 mg, 88%). 1H NMR (300 MHz, CDCl3) δ 7.59 (d, 1H, J = 15.5), 7.30 (d, 1H, J = 15.5), 6.85 (m, 1H), 6.73 (s, 2H), 5.95 (d, 1H, J = 9.7), 5.79 (s, 1H), 3.95 (m, 2H), 3.80 (d, 6H, J = 13.6), 2.38 (d, 2H, J = 6.1). 13C NMR (300 MHz, CDCl3) 169.01, 165.92, 147.18, 145.44, 144.34, 137.10, 126.63, 125.87, 119.61, 105.36, 56.36, 41.66, 24.83. HRMS (ESI/FT-MS): 304.1185 $[M+H]^+$; expected 304.1179.

(E)-1-(3-(4-(2-(2-ethoxyethoxy)ethoxy)-3,5-dimethoxyphenyl)acryloyl)-5,6-dihydropyridin-2(1H)-one (7)

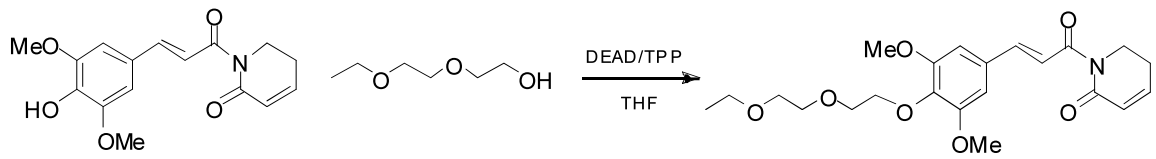

111 mg of (E)-1-(3-(4-hydroxy-3,5-dimethoxyphenyl)acryloyl)-5,6-dihydropyridin-2(1H)-one **(6)** (0.364 mmol, 1 eq.) and 143 mg TPP (0.546 mmol, 1.5 eq.), and 59 µL of 2-(2-ethoxyethoxy)ethanol (0.437 mmol, 1.2 eq.) were dissolved in 2.0 anhydrous THF under nitrogen at 0ºC. Then 87 µL of DEAD (0.546 mmol, 1.5 eq.) was slowly added to the solution. The mixture was slowly warmed to room temperature and stirred overnight. The crude reaction mixture was concentrated and directly purified by flash chromatography and HPLC to yield the pure product. (73.5 mg, 48.1%, after two purifications). 1H NMR (300 MHz, CDCl3) δ 7.59 (d, 1H, J = 15.6), 7.34 (d, 1H, J = 15.5), 6.87 (m, 1H), 6.71 (s, 2H), 5.96 (d, 1H, J = 9.7), 4.11 (m, 2H), 3.96 (t, 2H, J = 6.5), 3.78 (d, 6H, J = 10.6), 3.73 (t, 2H,

J = 5.2), 3.64 (dd, 2H, J = 3.7, 5.8), 3.52 (dd, 2H, J = 3.7, 5.9), 3.45 (q, 2H, J = 7.0), 2.40 (d, 2H, J = 6.2), 1.13 (t, 3H, J = 7.0). 13C NMR (300 MHz, CDCl3) 168.83, 165.80, 153.48, 145.49, 143.77, 139.15, 130.65, 125.80, 121.05, 105.60, 72.34, 70.66, 70.38, 69.89, 66.60, 56.18, 41.63, 24.80, 15.17. HRMS (ESI/FT-MS): 420.2020 $[M+H]^+$; expected 420.2017.

(E)-tert-butyl 3-(2-(2-(2-(2,6-dimethoxy-4-(3-oxo-3-(2-oxo-5,6-dihydropyridin-1(2H)-yl)prop-1-enyl)phenoxy)ethoxy)ethoxy)ethoxy)propanoate, (8)

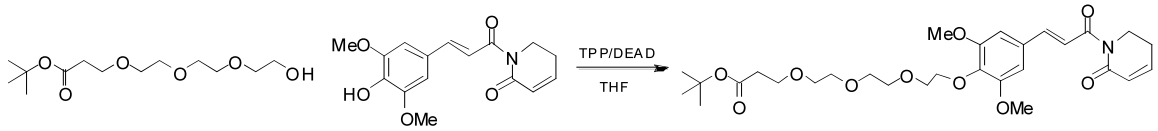

23.5 mg of (E)-1-(3-(4-hydroxy-3,5-dimethoxyphenyl)acryloyl)-5,6-dihydropyridin-2(1H)-one **(6)** (0.077 mmol, 1 eq.) and 30.5 mg TPP (0.116 mmol, 1.5 eq.), and 20 µL of tert-butyl 3-(2-(2-(2-hydroxyethoxy)ethoxy)ethoxy)propanoate (0.077 mmol, 1.0 eq.) were dissolved in 1.0 anhydrous THF under nitrogen at 0ºC. Then 18 µL of DEAD (0.116 mmol, 1.5 eq.) was slowly added to the solution. The mixture was slowly warmed to room temperature and stirred overnight. The crude reaction mixture was concentrated and directly purified by flash chromatography and HPLC to yield the pure product. (43.1 mg, 99%, after two purifications). 1H NMR (300 MHz, CDCl3) δ 7.67 (d, 1H, J = 15.6), 7.41 (d, 1H, J = 15.5), 6.95 (m, 1H), 6.78 (s, 2H), 6.04 (d, 1H, J = 9.7), 4.17 (m, 2H), 4.03 (t, 2H, J = 6.5), 3.86 (s, 6H), 3.79 (m, 2H), 3.65 (m, 10H), 2.49 (dd, 4H, J = 5.5, 7.7), 1.40 (s, 9H). 13C NMR (300 MHz, CDCl3) 170.88, 168.85, 165.82, 153.49, 145.56, 143.80, 130.66, 125.83, 121.05, 105.59, 80.46, 72.33, 70.66, 70.62, 70.53, 70.37, 66.89,

56.18, 41.64, 36.29, 28.10, 24.81. HRMS (ESI/FT-MS): 586.2626 $[M+Na]^+$; expected 586.2623.

(E)-3-(2-(2-(2-(2,6-dimethoxy-4-(3-oxo-3-(2-oxo-5,6-dihydropyridin-1(2H)-yl)prop-1-enyl)phenoxy)ethoxy)ethoxy)ethoxy)propanoic acid, (9)

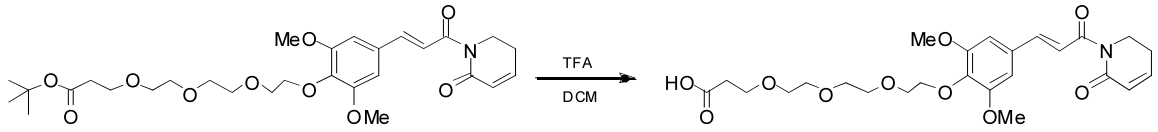

315 mg of (E)-tert-butyl 3-(2-(2-(2-(2,6-dimethoxy-4-(3-oxo-3-(2-oxo-5,6-dihydropyridin-1(2H)-yl)prop-1-enyl)phenoxy)ethoxy)ethoxy)ethoxy)propanoate **(8)** was dissolved in 9.0 mL DCM and then 3.0 mL of TFA was added at 0ºC. The reaction was stirred at 0ºC for 30 min and then 1 hour at room temperature. The reaction mixture was then concentrated and the product was isolated by flash chromatography and HPLC. (238.6mg, 84%). 1H NMR (300 MHz, CDCl3) δ 9.19 (b, 1H), 7.66 (d, 1H, J = 15.6), 7.40 (d, 1H, J = 15.5), 6.95 (m, 1H), 6.78 (s, 2H), 6.04 (d, 1H, J = 9.7), 4.17 (m, 2H), 4.03 (t, 2H, J = 6.5), 3.85 (s, 6H), 3.81 (m, 10H), 3.63 (s, 2H), 2.61 (t, 2H, J = 6.2), 2.47 (d, 2H, J = 6.2). 13C NMR (300 MHz, CDCl3) 168.92, 165.91, 153.43, 145.64, 143.84, 139.02, 130.67, 125.76, 121.05, 111.85, 105.61, 72.31, 70.62, 70.57, 70.39, 66.46, 56.19, 41.67, 34.92, 24.80. HRMS (ESI/FT-MS): 530.2003 $[M+Na]^+$; expected 530.1997.

General procedure for immobilization of bait molecule ((E)-3-(2-(2-(2-(2,6-dimethoxy-4-(3-oxo-3-(2-oxo-5,6-dihydropyridin-1(2H)-yl)prop-1-enyl)phenoxy)ethoxy)ethoxy)ethoxy)propanoic acid**, (9)**)

1) Solid-phase (beads) preparation: The solid-phase beads used in small molecule immobilization and affinity chromatography is Affigel 102 (Bio-Rad) with loading level of 12 μmol/mL suspension. 1.0 mL bead suspension was transferred to a 2.0 mL epi vial. The beads were washed with 3x 1.5 mL H_2O and 3 x 1.5 mL DMSO. The beads were then suspended in 0.5 mL anhydrous DMSO.

2) Bait molecule activation:

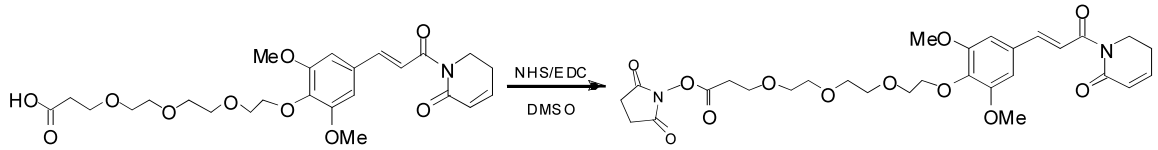

9.9 mg of linker-attached piperlongumine (E)-3-(2-(2-(2-(2,6-dimethoxy-4-(3-oxo-3-(2-oxo-5,6-dihydropyridin-1(2H)-yl)prop-1-enyl)phenoxy)ethoxy)ethoxy)ethoxy)propanoic acid **(9)** (0.020 mmol, 1.0 eq.), 2.69 mg of NHS (0.023 mmol, 1.2 eq.), and 5.61 mg of EDC (0.029 mmol, 1.5 eq.) were dissolved in 0.2 mL of anhydrous DMSO. The activation reaction was stirred at room temperature and monitored by LC-MS after 2 hours, the activation was completed.

3) Bait molecule immobilization:

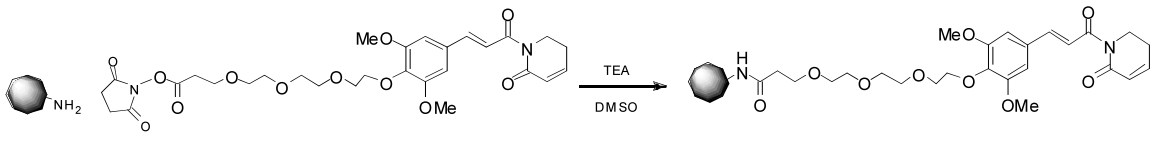

The activated bait molecule solution was directly added to the bead suspension prepared based on specific loading levels (6.25%, 12.5% and 25.0%,

respectively). After adding the activation solutions, 14 µL of TEA (0.098 mmol, 5.0 eq.) was added to each reaction. The reaction vials were gently vortexed at room temperature for 1 hour. LC-MS was used to monitor the depletion of the activated acid.

4) Work-up: After the immobilization, the vials were centrifuged. The supernatant was removed and the beads were washed with 3 x 2 mL DMSO and 3 x 2 mL H_2O. The beads were subsequently suspended in 1x PBS (0.8 mL) and stored at 4 ºC before use.

SILAC media preparation and cell culture conditions. We followed all standard SILAC media preparation and labeling steps as previously described[11]. Briefly, 30 mg/L of L-methionine and glucose (final concentration of 4.5g/L) was added to base media according to standard formulations for high glucose DMEM (DMEM/high). This base media was divided into two and either 'light' forms of arginine and lysine or 'heavy' L-arginine-U-13C6 (28 mg/L) and L-lysine-13C615N2 (146mg/L) was added to generate the two SILAC labeling mediums. Each medium with the full complement of amino acids was sterile filtered through a 0.22µ filter (Milipore, Bedford MA). EJ and U2OS cells were grown in DMEM/high labeling media, prepared as described above, supplemented with 2 mM L-glutamine, and 5% dialyzed fetal bovine serum plus antibiotics, in a humidified atmosphere with 5% CO_2 in air. Cells were grown for at least six cell divisions in labeling media.

Biochemical purification with small molecule affinity matrices. Separate cultures of EJ or U2OS cells SILAC labeled either with L-arginine and L-lysine (light) or L-arginine-13C6 and L-lysine-13C6-15N2 (heavy) were lysed in ice-chilled ModRIPA buffer containing 1% NP-40, 0.1% Na deoxycholate, 150 mM NaCl, 1mM EDTA, 50 mM Tris, pH 7.5, and protease inhibitors (CompleteTM tablets, RocheApplied Science, Indianapolis, IN). Lysates were vortexed intermittently while chilled on ice for 10 min and clarified by spinning at 14,000 x g. Protein concentrations of light and heavy lysates were estimated with the Protein Assay Dye Reagent Concentrate (Biorad, Hercules CA) and equalized. The protein concentrations of lysates varied between 1.7 to 2.2 mg/mL, affinity enrichments were performed in lysate volumes of 1.4 mL in a 1.5 mL microcentrifuge tube.

PL (in DMSO) at 70, 14 and 7 fold excess over the amount of PL on beads for EJ cells and 100, 21 and 11 fold excess for U2OS cells was added to 2 mg of light EJ or U2OS lysate. An equal volume of DMSO was then added to 2 mg of heavy EJ or U2OS cells as a control. Thirty microliters of a 50% slurry in phosphate buffered saline (PBS) of PL-bead was added to both light and heavy lysates. Affinity enrichments were incubated overnight (approx. 16 hrs) on an end-over-end rotator at 4°C. Following incubation, the tubes were spun at 1000 x g on a benchtop centrifuge to pellet the beads. The supernatant was aspirated, taking care to avoid disturbing the beads. Each tube in a set was washed with ModRIPA buffer twice to remove excess soluble small molecule competitor. Beads from the

two tubes were then combined for an extra washing step in ModRIPA. After the third and final wash, beads were collected by spinning at 1000 x g and the wash aspirated leaving approximately 20 µL of buffer in the tube.

1D-SDS-PAGE and MS analysis. Proteins enriched in SILAC affinity pull-downs were reduced and alkylated, on bead, in 2 mM DTT and 10 mM iodoacetamide respectively. One part LDS buffer (Invitrogen) was added to three parts sample (including beads) and tubes heated to 70°C for 10 minutes. Proteins were resolved on a 4-12% gradient 1.5 mm thick Bis-Tris gel with MES running buffer (Nupage, Invitrogen) and Coomassie stained (Simply Blue, Invitrogen). Gel lanes were excised into six pieces and then further cut into 1.5 mm cubes. The gel pieces were further destained in a solution containing 50% EtOH and 50% 50 mM ammonium bicarbonate, then dehydrated in 100% EtOH before addition of sufficient trypsin (12.5 ng/µL) to swell the gel pieces completely. An additional 100 µL of 50 mM ammonium bicarbonate was added before incubating at 37°C overnight on a thermomixer (Eppendorf). Enzymatic digestion was stopped by the addition of 100 µL of 1% TFA to tubes. A second extraction with 300 µL of 0.1% TFA was combined with the first extract and the peptides from each gel slice cleaned up on C18 StageTips[32]. Peptides were eluted in 50 µL of 80% acetonitrile/0.1% TFA and dried down in a evaporative centrifuge to remove organic solvents. The peptides were then resuspended by vortexing in 7 µL of 0.1% TFA and analyzed by nanoflow-LCMS with an Agilent 1100 with autosampler and a LTQOrbitrap. Peptides were resolved on a 10 cm column,

made in-house by packing a self pulled 75 µm I.D. capillary, 15 µm tip (P-2000 laser based puller, Sutter Instruments) column with 3 µm Reprosil-C18-AQ beads (Dr. Maisch GmbH, Ammerbuch-Entringen, Germany) with an analytical flowrate of 200 nL/min and a 58min linear gradient (~ 0.57 %B/min) from 0.1% formic acid in water to 0.1% formic acid/90% acetonitrile. The run time was 108 min for a single sample, including sample loading and column reconditioning.

We used a MS method with a master Orbitrap full scan (60,000 resolution) and data dependent LTQ MS/MS scans for the top five precursors (excluding z=1) from the Orbitrap scan. Each cycle was approximately 2 secs long. MS raw files were processed for protein identification and quantitation using extract_msn.exe (Thermo, Bremen Germany), Mascot (Ver. 2.1.03 Matrixscience, London UK), and academic software, DTASupercharge and MSQuant (CEBI, open-source http://msquant.sourceforge.net). MS/MS peak lists in Mascot Generic Format were generated using extract_msn.exe and DTASupercharge and searched with Mascot using IPI human ver.3.32 (http://ebi.ac.uk) with a concatenated decoy database containing randomized sequences from the same database. Common contaminants like bovine serum albumin, trypsin etc. were also added to the database. Variable modifications used were oxidized methionine, arginine-13C6, lysine-13C6 15N2, and carbamidomethyl-cysteine was a fixed modification. The precursor mass tolerance used in the search was 15 ppm and fragment mass tolerance was 0.7 Da. Proteins with a minimum Mascot score of 66 (at least 1 peptide with score > 66) and peptides with score > 20 were quantified by MSQuant. Only proteins with a minimum of two quantifiable peptides were

included in our dataset. The false positive rate for protein identification is < 1 % and < 5% at the peptide level, as determined using the decoy database strategy.

Statistical analysis of SC experiments. To model log2 protein ratio values, we adapted the empirical “Bayes” framework to compute the posterior probability that a ratio value arises from the null distribution (Margolin, et al. manuscript in preparation). Briefly, by application of Bayes’ theorem, this quantity is computed as $Pr(Z = 0 \mid X) = [Pr(X \mid Z = 0)Pr(Z = 0)]/Pr(X)$where Z is a binary variable taking the value of one if the protein is bound by the compound, and X is a measured log2 SILAC ratio. We model Pr(X) using a Gaussian kernel estimator with pareto distributions fit to 5% of the data at either tail, to avoid unreliable estimation in regions of data sparsity. The distribution for $Pr(X \mid Z = 0)Pr(Z = 0)$ is then inferred by fitting a Gaussian distribution using only the portion of $Pr(X)$ arising from the central two thirds of the data.

SUPPLEMENTARY FIGURES AND LEGENDS

Supplementary Table 1: Summary of Clinical Observation of PL in Rat*

Group (6 rats)	Dosing route	Dosage (mg/kg)	Clinical Observation
1	**PO**	**100**	All animals were observed with prolonged inactivity at approximately 15 mins, eye covering at approximately 18 mins, prostate from 15 mins to 22 mins, and almost recovered at approximately 1 hr after dosing. One rat was observed with loose stools at approximately 3.5 hrs after dosing.
2	**PO**	**300**	All animals were observed with prolonged inactivity at approximately 5 mins, prostate and eye covering from 10 mins to 40 mins constantly, and almost recovered at approximately 2.5 hrs after dosing. One rat was observed with loose stools at approximately 3.5 hrs and watery feces at approximately 4 hrs after dosing.
3	**PO**	**1000**	All animals were observed with prolonged inactivity from 3 mins to 6 mins constantly, eye covering approximately 13 mins, and prostate at approximately 22 mins. And almost recovered at approximately at 2 hrs. One rat was observed with loss of skin elasticity at 40 mins and lasted 80 mins. All animals were observed with loose stool at approximately 4 hrs after dosing.
4	**PO**	**3000**	All animals were observed with prolonged inactivity at approximately 3 mins, prostate at approximately 40 mins. Two rats were observed with licking excessive at approximately 3 mins, two were observed with eye covering at 12 mins, one was observed with breathing rapid at approximately 24 mins, two were observed with loss of skin elasticity at approximately 30 mins, and two rats gradually recovered from 2 hrs. One rat was observed with watery stools at approximately 3 hrs, yellow and white mucoid feces at 4 hrs. One rat died at approximately 1 hr.

*Six Sprague Dawley Rats (male and female) were used for the study.

Supplementary Table 2: Summary of Clinical Observation of PL in CD-1 mouse

Group (6 mice)	Dosing route	Dosage (mg/kg)	Clinical Observation
1	**PO**	**100**	All animals were observed with prolonged inactivity about 12 mins, and almost recovered at approximately 22 mins after dosing.
2	**PO**	**300**	Two mice were observed with prolonged inactivity, eye covering at approximately 6 mins, all animals were observed with abdominal breathing from 10 mins to 40 mins constantly. And almost recovered from 90 mins to 110 mins constantly. One mouse was observed with watery feces at 3hrs after dosing.
3	**PO**	**1000**	All animals were observed with prolonged inactivity at approximately 3 mins, eye covering from 8 mins to 20 mins constantly, abdominal breathing from 8 mins to 35 mins constantly, prostrate from 17 mins to 30 mins constantly. One mouse was observed with breathing rapid at approximately 22 mins, irregular respiration at 45 mins. And all animals were almost recovered at 2 hrs after dosing. One mouse was observed with loose stools at approximately 3 hrs after dosing.
4	**PO**	**2000**	All animals were observed with prolonged inactivity, eye covering at approximately 4 mins, prostrate at approximately 12 mins, abdominal breathing from 9mins to20mins constantly. One mouse was observed with body cold to touch at approximately 70 mins. Two mice were observed with loose stools at 2 hrs, and one of the mice was observed with watery feces at 3 hrs after dosing. One mouse was observed with material round eyes and panting at 40 mins, tremor at 140 mins and lasted 10 mins. And all animals were gradually recovered from 140 mins after dosing.
5	**PO**	**3000**	All animals were observed with prolonged inactivity at approximately 2 mins, eye covering and abdominal breathing at 10 mins, prostrate from 10 mins to 21 mins, body cold to touch at 80 mins. Two mice were observed with loose stool at 3 hrs, and one of the mice was observed with watery stool at 4 hrs. One mouse was observed with tremor at approximately 140 mins, twitching and righting reflex lost, gasping from 200 mins to 210 mins, and dead at 213 mins. The remaining mice gradually recovered from 3 hrs after dosing.

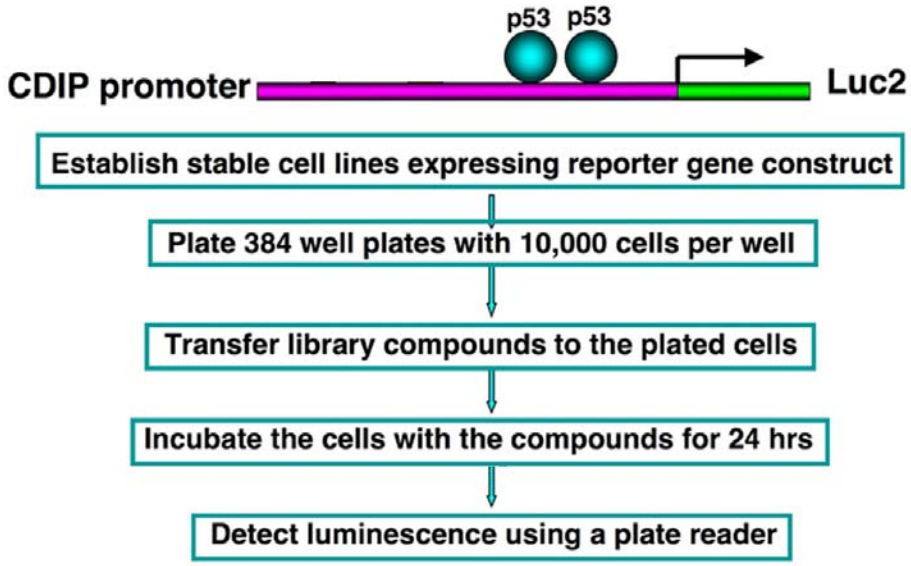

Supplementary Figure 1. An overview of the screening method. A reporter construct was created that included the human CDIP promoter carrying p53-responsive elements operatively linked to the firefly *luc2* reporter gene. U2OS cell-lines stably expressing the CDIP reporter construct were generated. Cells were plated in 30µl of medium containing 10,000 cells per well into 384-well pates using automated plate filler. Twenty-four hours after plating, small molecule library test compounds were pin transferred from stock plates to the 384-well assay plates containing cells. The assay plates were incubated with the compounds for 24 hours, following which 30µl of the steadylite HTS reagent was added using automated plate filler. Luminescence was measured with an automated plate reader after shaking the assay plates at room temperature for 15 minutes to allow full signal generation from the lysed cells (the screen was done in two replicates).

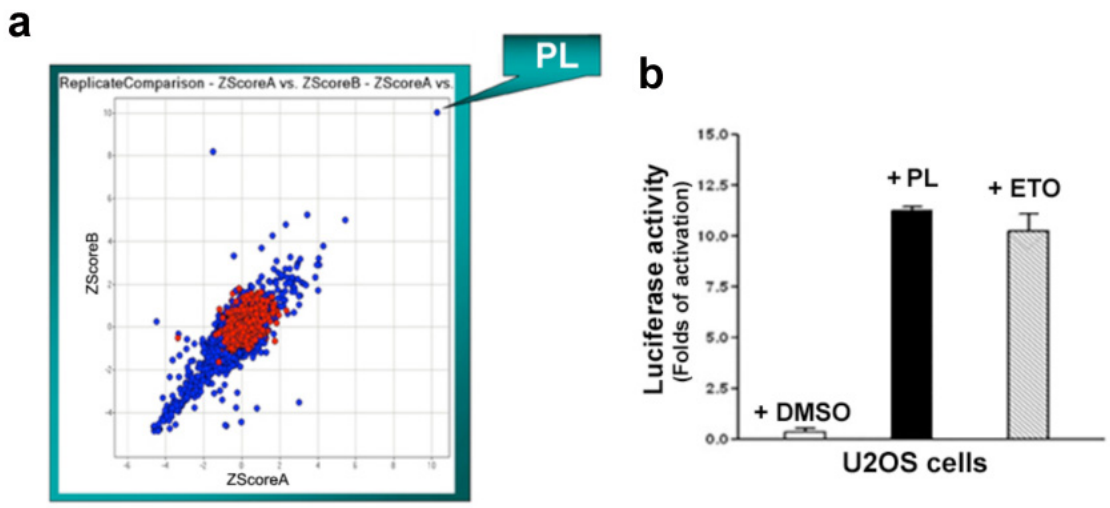

Supplementary Figure 2. Identification of a CDIP-activating compound.

(a) Composite Z score analyzed by Spotfire data analysis. The results of the initial screen were analyzed using Spotfire software to identify compounds that activated p53-responsive reporter expression at 24 hours. The "Z-scoreA" and "Z-scoreB" represents the Z scores for the two independent replicates of the screen. On the XY-scatter plot, the red dots indicate DMSO treatment and the blue dots indicate the test compounds. **(b)** PL compound (10 μM) stimulates luciferase activity of CDIP promoter containing p53-binding sites in U2OS cells. Etoposide (ETO, 25 μM) was used as a positive control. Each bar represents the mean ± S.D. of three separate experiments.

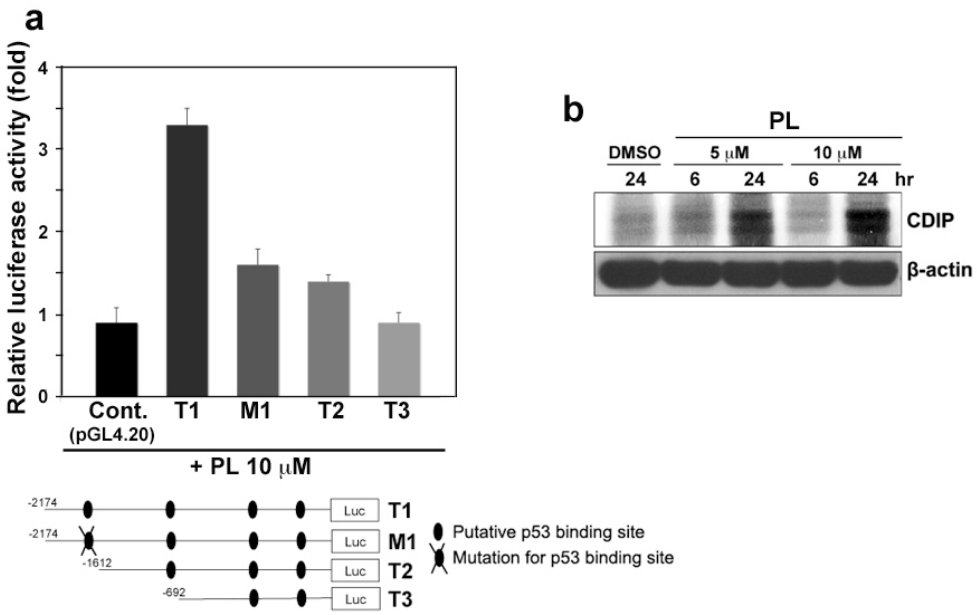

Supplementary Figure 3. PL mediated induction of CDIP in U2OS cells (a) Putative p53 binding sites (p53-BS) on the CDIP promoter were previously identified in our lab [1]. The wild-type promoter (T1), two truncated forms of the promoter (T2 and T3) and a promoter with mutated p53 binding sites (M1), were all cloned into pGL4.20. U2OS cells were cotransfected with either one of the CDIP promoter constructs or the empty vector (pGL4.20) and pRL-SV40 *Renilla* luciferase construct (for normalization). Twenty fours after transfection U2OS cells were then treated with DMSO or PL (10μM) for 16 hrs. Relative luciferase activity from three independent experiments is shown for each construct as fold change compared to DMSO used as a control. **(b)** PL mediated induction of CDIP protein expression in U2OS cells. U2OS cells were treated with PL at two different concentrations (5μM and 10μM) for 6 and 24 hours. The induction of endogenous CDIP protein was detected by western blot analysis using anti-CDIP antibody and β-actin as the loading control.

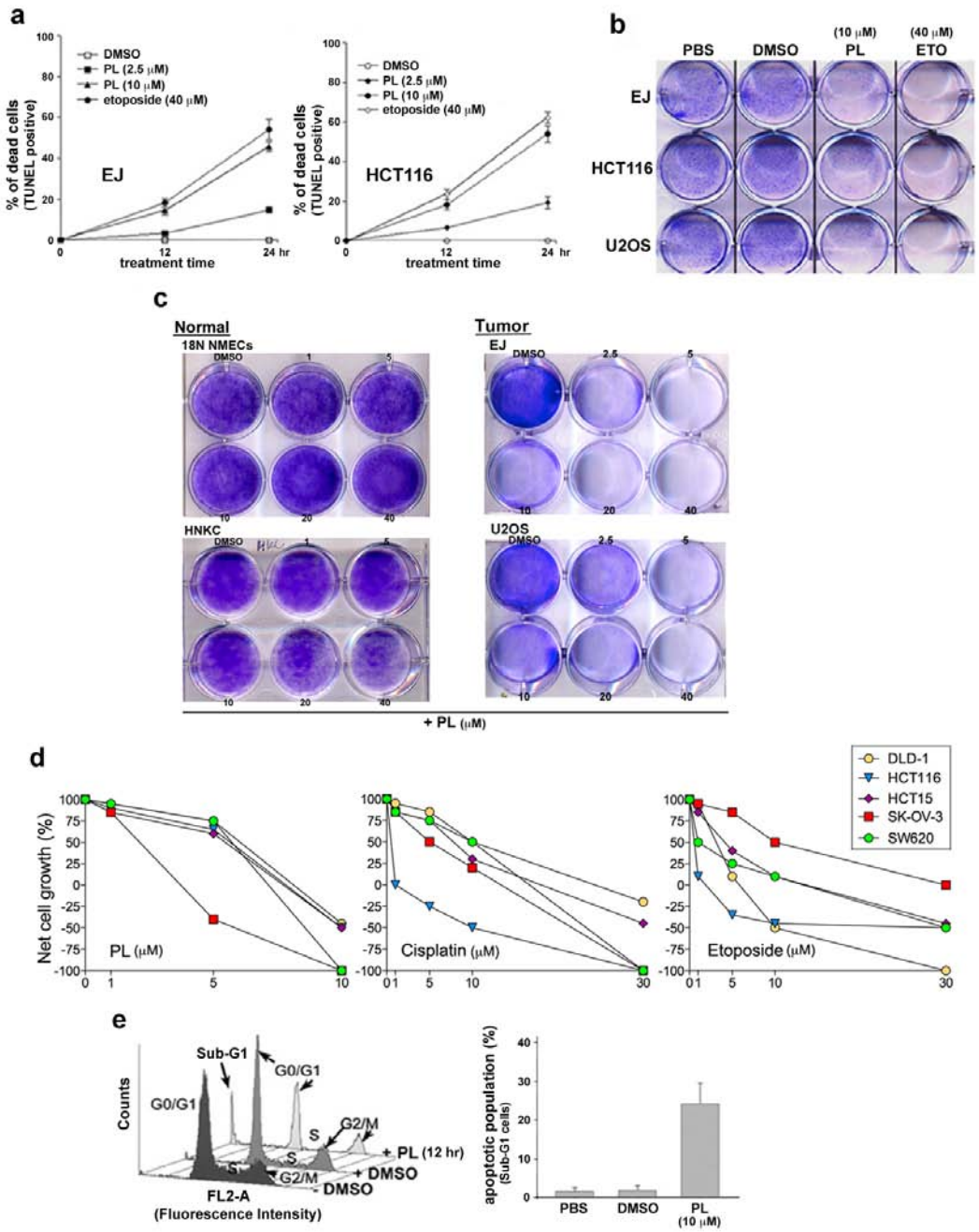

Supplementary Figure 4. Antiproliferative and cytotoxic activity of PL on human cancer cells. (a) Quantification of apoptotic cells determined by TUNEL assay. PL treatment induces cell death in human bladder cancer (EJ) and in human colon cancer (HCT116) cells in a dose-dependent and time-dependent manner. Etoposide, a genotoxic agent, was used as a positive control at 40μM

concentration. TUNEL-positive cell fractions were measured by flow cytometry and compared with DMSO treated controls **(b)** Crystal violet cell viability staining of EJ, HCT116 and U2OS cells after PL treatment. **(c)** Selective killing of tumor cells by PL in a dose-dependent manner. Normal and tumor cells were treated with PL at 1-40 μM concentrations for 24 hours, and live cells were stained by crystal violet. DMSO was used as control solvent. PL exhibited cytotoxicity only in tumor cells (EJ and U2OS) and not in normal human breast epithelial cells (18N) and human normal keratinocyte cells (HNKC) at less than 15 μM concentration. At higher concentration of PL (>40 μM) slight cytotoxicity was observed in normal cells. Normal cells were grown in the respective growth media in 6 well tissue-culture plates to ~80% confluency. Note that PL is effective in killing cancer cells at concentrations less than 15 μM. **(d)** Dose-response curves of human colon and ovarian cancer cells treated with PL. Several human colon cancer cell lines (DLD-1, HCT116, HCT-15 and SW480) an ovarian cancer cell line (SK-OV-3) were treated with PL at the denoted concentrations. Forty-eight hours after treatment, cell viability was assessed by SRB (sulforhodamine B) assay. For each experiment, cell toxicity was calculated by comparing the number of cells surviving at time zero with those surviving at the end of the experiment. Each data point represents the mean of three independent experiments. Note that PL was found to be more effective in killing cancer cells compared with other chemotherapy drugs, such as etoposide and cisplatin. **(e)** FACS-PI analysis of PL treated HCT116 colon cancer cells. PL treatment results in an increase of the sub-G1 apoptotic population by 25-30% as indicated (mean ± SD of three

experiments).

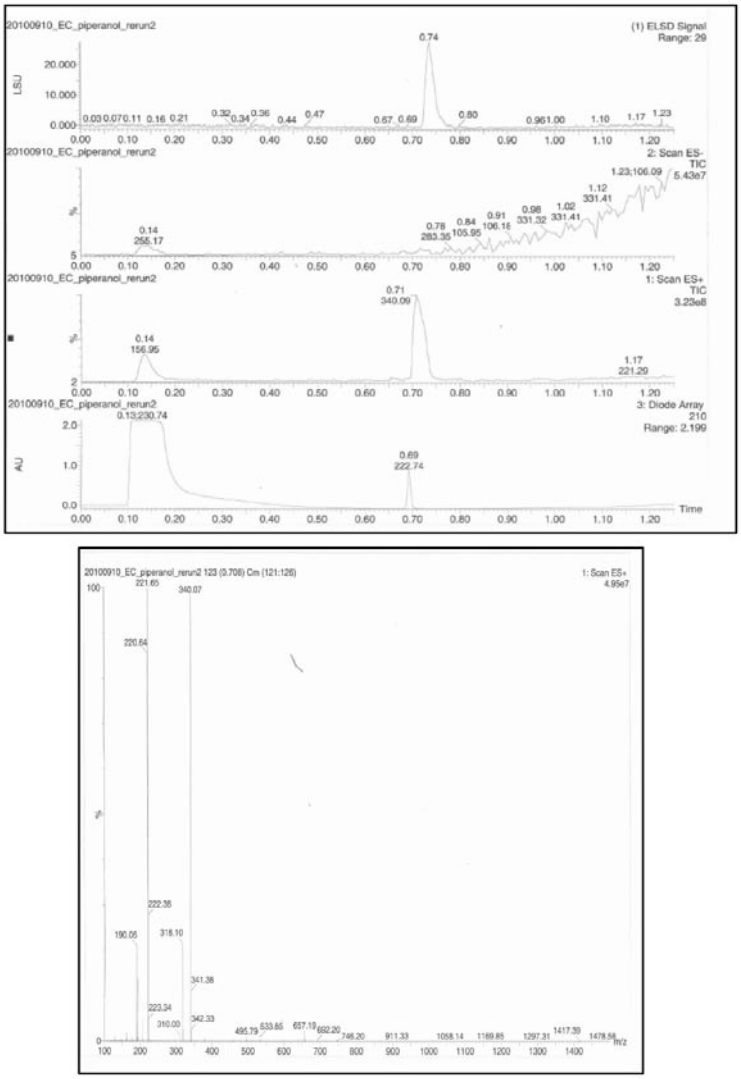

Supplementary Figure 5. Compound purity was determined by UPLC-MS by UV absorbance at 210 nm. Identity was determined on a SQ mass-spectrometer by positive electrospray ionization. Mobile phase A consisted of 0.1% ammonium hydroxide in water while mobile phase B consisted of 0.1% ammonium hydroxide in acetonitrile. The gradient ran from 5% to 95% mobile phase B over 0.8 minutes. An Acquity BEH C18, 1.7um, 1.0 x 50 mm column was used with column temperature maintained at 65^{o}C. Compound was dissolved in DMF.

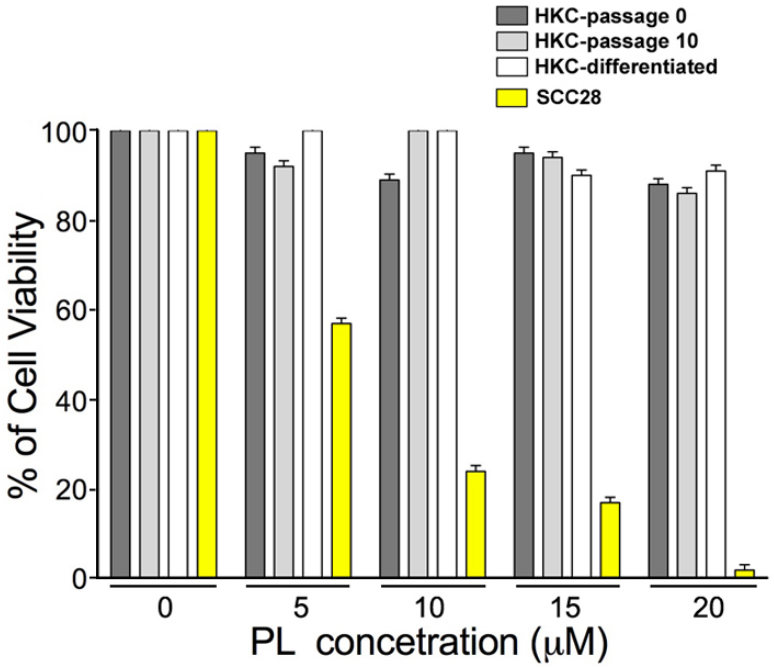

Supplementary Figure 6. The effect of PL in proliferating, non-proliferating and non-dividing differentiated human normal keratinocytes. PL effects were assessed in primary human keratinocytes grown in 6 well tissue culture plates on collagen at 80% confluency in passage 0 (highly proliferating); passage 10 (decrease ability to proliferate) as well as in "differentiation"-inducing conditions when compared to keratinocyte-derived squamous cell carcinoma cells. These cells were treated with PL for 24 hours at 0-20 μM followed by cell death measurement (a mean of three independent experiments). Cytotoxicity was measured by trypan-blue exclusion assay. We chose to use adherent keratinocytes (passage 0 and 10) versus cells in suspension since loss of adhesion to the substrate triggers important features of terminal differentiation in keratinocytes, including irreversible withdrawal from the cell cycle and inhibition of proliferation. Normal keratinocytes and SCC28 were grown in the same keratinocyte growth medium (Invitrogen).

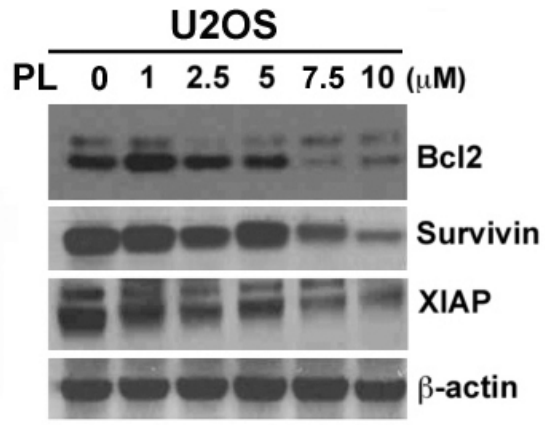

Supplementary Figure 7. The effects of PL on pro-survival proteins. Expression of pro-survival proteins were measured by western blot analyses of Bcl2, survivin and XIAP in PL-treated U2OS cells. β-actin expression was used as a loading control.

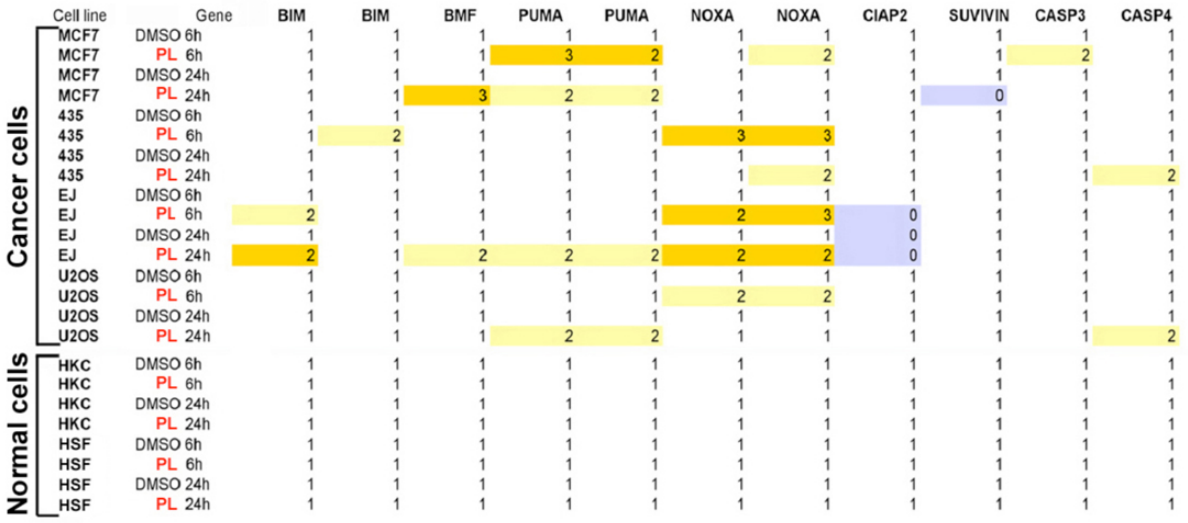

	Cell line	Gene	BIM	BIM	BMF	PUMA	PUMA	NOXA	NOXA	CIAP2	SUVIVIN	CASP3	CASP4
Cancer cells	MCF7	DMSO 6h	1	1	1	1	1	1	1	1	1	1	1
	MCF7	PL 6h	1	1	1	3	2	1	2	1	1	2	1
	MCF7	DMSO 24h	1	1	1	1	1	1	1	1	1	1	1
	MCF7	PL 24h	1	1	3	2	2	1	1	1	0	1	1
	435	DMSO 6h	1	1	1	1	1	1	1	1	1	1	1
	435	PL 6h	1	2	1	1	1	3	3	1	1	1	1
	435	DMSO 24h	1	1	1	1	1	1	1	1	1	1	1
	435	PL 24h	1	1	1	1	1	1	2	1	1	1	2
	EJ	DMSO 6h	1	1	1	1	1	1	1	1	1	1	1
	EJ	PL 6h	2	1	1	1	1	2	3	0	1	1	1
	EJ	DMSO 24h	1	1	1	1	1	1	1	0	1	1	1
	EJ	PL 24h	2	1	2	2	2	2	2	0	1	1	1
	U2OS	DMSO 6h	1	1	1	1	1	1	1	1	1	1	1
	U2OS	PL 6h	1	1	1	1	1	2	2	1	1	1	1
	U2OS	DMSO 24h	1	1	1	1	1	1	1	1	1	1	1
	U2OS	PL 24h	1	1	1	2	2	1	1	1	1	1	2
Normal cells	HKC	DMSO 6h	1	1	1	1	1	1	1	1	1	1	1
	HKC	PL 6h	1	1	1	1	1	1	1	1	1	1	1
	HKC	DMSO 24h	1	1	1	1	1	1	1	1	1	1	1
	HKC	PL 24h	1	1	1	1	1	1	1	1	1	1	1
	HSF	DMSO 6h	1	1	1	1	1	1	1	1	1	1	1
	HSF	PL 6h	1	1	1	1	1	1	1	1	1	1	1
	HSF	DMSO 24h	1	1	1	1	1	1	1	1	1	1	1
	HSF	PL 24h	1	1	1	1	1	1	1	1	1	1	1

Supplementary Figure 8. Expression profiling of PL-responsive gene transcripts involved in cell death/apoptosis using LUMINEX. To understand the transcriptional signature of PL-treated cells, we selected 55 genes involved either in the apoptotic or pro-survival responses of cancer and normal cells and measured their mRNA levels upon PL treatment using an approach in which multiplexed ligation-mediated amplification products can be detected by bead-based flow cytometry [2]. Four different types of cancer cells (MCF7, MDAMBA435, EJ and U2OS) and two different types of normal cells (fibroblasts and primary human keratinocytes) were treated with 10 μM PL for either 6 or 24 h and compared to the respective DMSO controls. Several pro-apoptotic genes like Bim, PUMA and Noxa were upregulated at 6 and 24 h after PL treatment in the cancer cells while survival genes showed significantly reduced mRNA levels. A comparison with other pro-apoptotic gene signatures in the Connectivity Map [3] showed top-ranked scores of PL for the induction of pro-apoptotic molecules

such as NOXA. Human normal (HKC: human normal keratinocytes; and HSF: human skin fibroblasts) and tumor cancer cells treated with PL (10 μM) were lysed, and lysates were transferred to a 384-well plate coated with oligo-dT. Reverse transcription was performed and probes were hybridized to the cDNA. Amplicons are stained with streptavidin-phycoerythrin and quantified with dual-color flow cytometry. Bead color was used to identify each gene. The amount of phycoerythrin fluorescence measures the quantity of transcript; mRNA levels for representative genes are shown as fold change relative to 1.

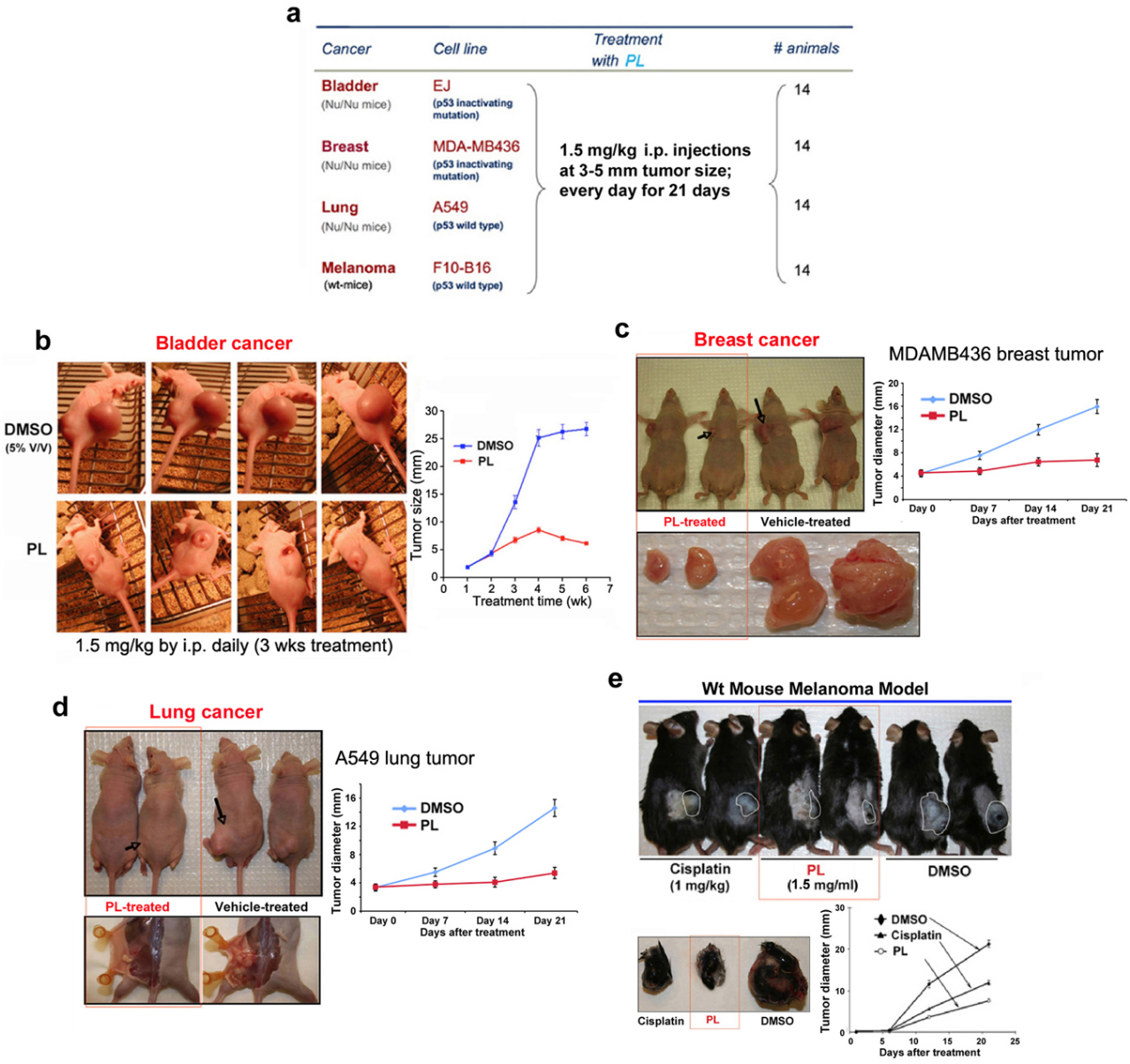

Supplementary Figure 9. Anti-tumor effect of PL in bladder cancer, breast cancer, lung cancer and melanoma xenograft mouse models. (a) Tumor models used in this study. **(b)** Therapeutic activity of PL in xenograft tumor mice bearing EJ bladder cancer cells. 24 nude mice were injected with $2x10^6$ EJ cells subcutaneously on the flanks. 12 mice were used in each group (control and PL). When tumor mass reached ~3 mm, mice were treated i.p. with 37.5 µg of PL (1.5

mg/kg/day) per mouse. **(c)** Breast cancer model using MDAMB436 cells. After 3 weeks, tumor masses were excised and measured. **(d)** Lung cancer model using A549 human lung cancer cells. After 3 weeks treatment, tumor sizes were measured. **(e)** Melanoma model using F10-B16 murine melanoma cells. B16 cells (1 million cells) were injected subcutaneously. When the tumor size reached ~1 mm the animals were treated PL for 21 days. Cisplatin was used as a positive control and DMSO was used as the vehicle.

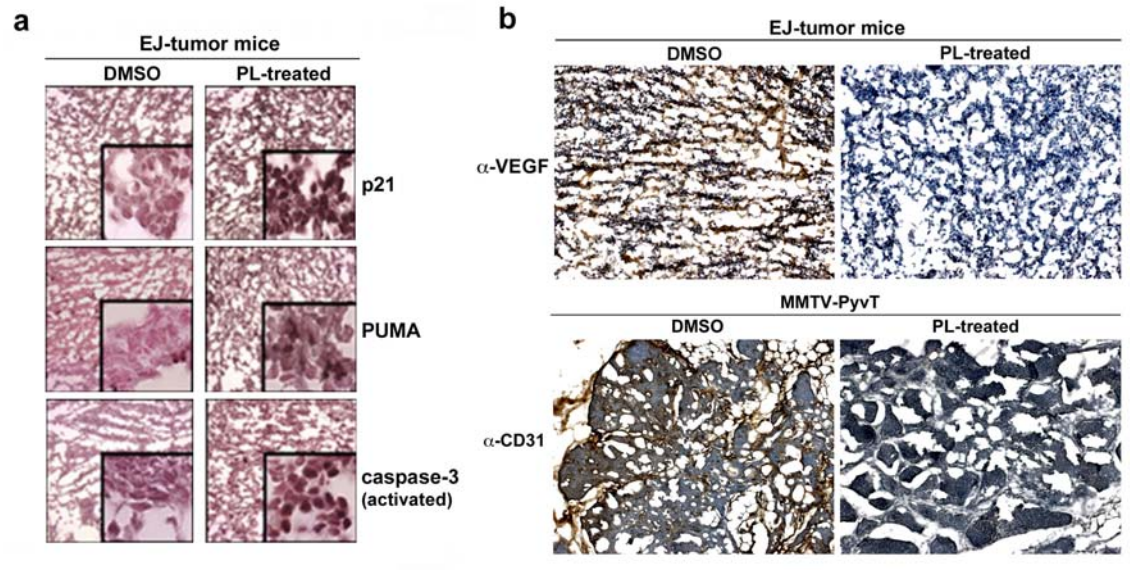

Supplementary Figure 10. Staining of blood vessel markers. EJ-tumor mice were treated with PL (1.5 mg/kg/day) or DMSO for 3 weeks. Following treatment, tumors from each group were excised and tissue sections were subjected to immunohistochemistry detection using the indicated antibodies. **(a)** Expression analysis of PUMA, p21 and caspase-3 (activated) by immunohistochemistry. **(b)** VEGF expression of PL-treated mice. The DMSO-treated tumor sections showed high expression of VEGF on blood vessel structure, but no significant level of staining was observed in the PL-treated tissue sections. **(c)** CD31f staining in PL-treated MMTV-PyVT mouse tumor samples. Tumor vasculatures of the DMSO and PL-treated samples were visualized by immmunohistochemistry (nuclei were counterstained by haematoxylin) using anti-CD31 antibodies (BD Pharmigen). PL-treated tumor samples did not exhibit CD31 staining while DMSO treated tumor samples showed high CD31 staining.

a

	$AUC_{(0-t)}$	$AUC_{(0-\infty)}$	$MRT_{(0-\infty)}$	$t_{1/2}$	T_{max}	Vz	CLz	C_{max}
	µg/L*hr	µg/L*hr	hr	hr	hr	L/kg	L/hr/kg	µg/L
IV								
5 mg/kg	280.73	283.01	0.30	0.95	0.083	24.28	17.67	905.62
10 mg/kg	516.62	535.04	0.51	1.60	0.083	43.25	18.69	1658.61
PO								
5 mg/kg	214.12	216.18	0.95	1.42	0.083	NA	NA	884.31
10 mg/kg	266.69	267.92	1.99	0.84	0.083	NA	NA	201.42

b

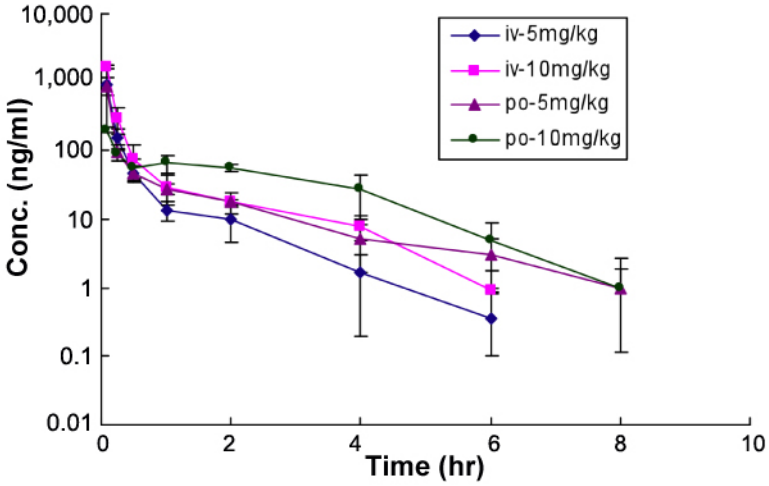

Supplementary Figure 11. The Pharmacokinetic characteristics of PL in C57BL/6 mice. (a) Selected Pharmacokinetics Parameters of PL in C57BL/6 mice following intravenous (iv) and oral (po) administration. **(b)** Plasma concentration-time curve of PL in C57BL/6 mice following intravenous and oral administration (mean ± SD, n=3). Following IV injection of PL at 5 mg/kg, the value of systemic clearance was 17.67 L/hr/kg, which corresponded to 3.27-fold of mouse hepatic blood flow. The values of half-life and V_z were 0.95 hr and 24.28 L/kg. Following IV injection at 10 mg/kg, the value of systemic clearance was 18.69 L/hr/kg, which corresponded to 3.46-fold of mouse hepatic blood flow.

The values of half-life and V_z were 1.60 hr and 43.25 L/kg. The bioavailability of PL following oral administration at 5 mg/kg and 10 mg/kg were 76.39% and 50.08%, respectively.

CD-1 Mouse Hematology

Test Name	(test units)	Reference Range Low - High	**Control** (Mean)	**PL treated** (Mean)
WBC	(10^3/µl)	2.6 - 12	8.2 ± 0.446	8.88 ± 0.702
LYM	(10^3/µl)	1.3 - 9	6.3 ± 0.326	7 ± 0.584
MONO	(10^3/µl)	0.1 - 0.5	0.433 ± 0.021	0.56 ± 0.04
GRAND	(10^3/µl)	0.4 - 2.5	1.183 ± 0.06	1.56 ± 0.129
LYM%	(%)	0 - 99.9	80.067 ± 0.884	73.5 ± 3.156
MONO%	(%)	0 - 99.9	4.783 ± 0.357	5.95 ± 0.354
GRAN	(%)	0 - 99.9	15.15 ± 0.554	20.55 ± 2.9
HCT	(%)	32 - 48	45.517 ± 0.554	48.383 ± 2.598
MCV	(fl)	42 - 55	49.8 ± 0.677	53.55 ± 1.946
RDWa	(fl)	0 - 99.9	34.717 ± 0.745	36.183 ± 0.896
RDW	(%)	0 - 99.9	19.033 ± 0.198	18.067 ± 0.53
HGB	(g/dl)	10.1 - 16.1	15.617 ± 0.56	15.483 ± 0.491
MCHC	(g/dl)	29 - 35	34.383 ± 0.199	32.233 ± 1.139
MCH	(pg)	13 - 18.1	17.083 ± 0.261	17.15 ± 0.05
RBC	(10^6/µl)	6.5 - 10.1	9.122 ± 0.201	9.015 ± 0.276
PLT	(10^3/µl)	300 - 1500	1124 ± 134.07	1006 ± 103.13
MPV	(fl)	0 - 99.9	5.633 ± 0.203	5.9 ± 0.216

Supplementary Figure 12. Mouse hematology with or without PL treatment. The CD-1 mice were administered PL (2.4mg/kg) or the vehicle, intraperitoneally, for 6 days. Blood samples were obtained from the facial vein of the animals and whole blood was analyzed using an automated hematology analyzer by the Massachusetts General Hospital veterinary clinical pathology services. The mean values of white blood cell (WBC), lymphocytes (LYM), monocytes (MONO), granulocytes (GRAND), hematocrit (HCT), mean corpuscular volume (MCV), red

blood cell distribution width absolute (RDWa), red blood cell distribution width (RDW) hemoglobin (HGB), mean cell hemoglobin concentration (MCHC), mean cell hemoglobin (MCH), red blood cell (RBC), platelet count (PLT) and mean platelet volume (MPV) of the control and PL treated animals are presented in the table. The results from the standard hematological evaluation did not reveal any significant difference between the control and PL treated groups. Normal reference ranges are also shown.

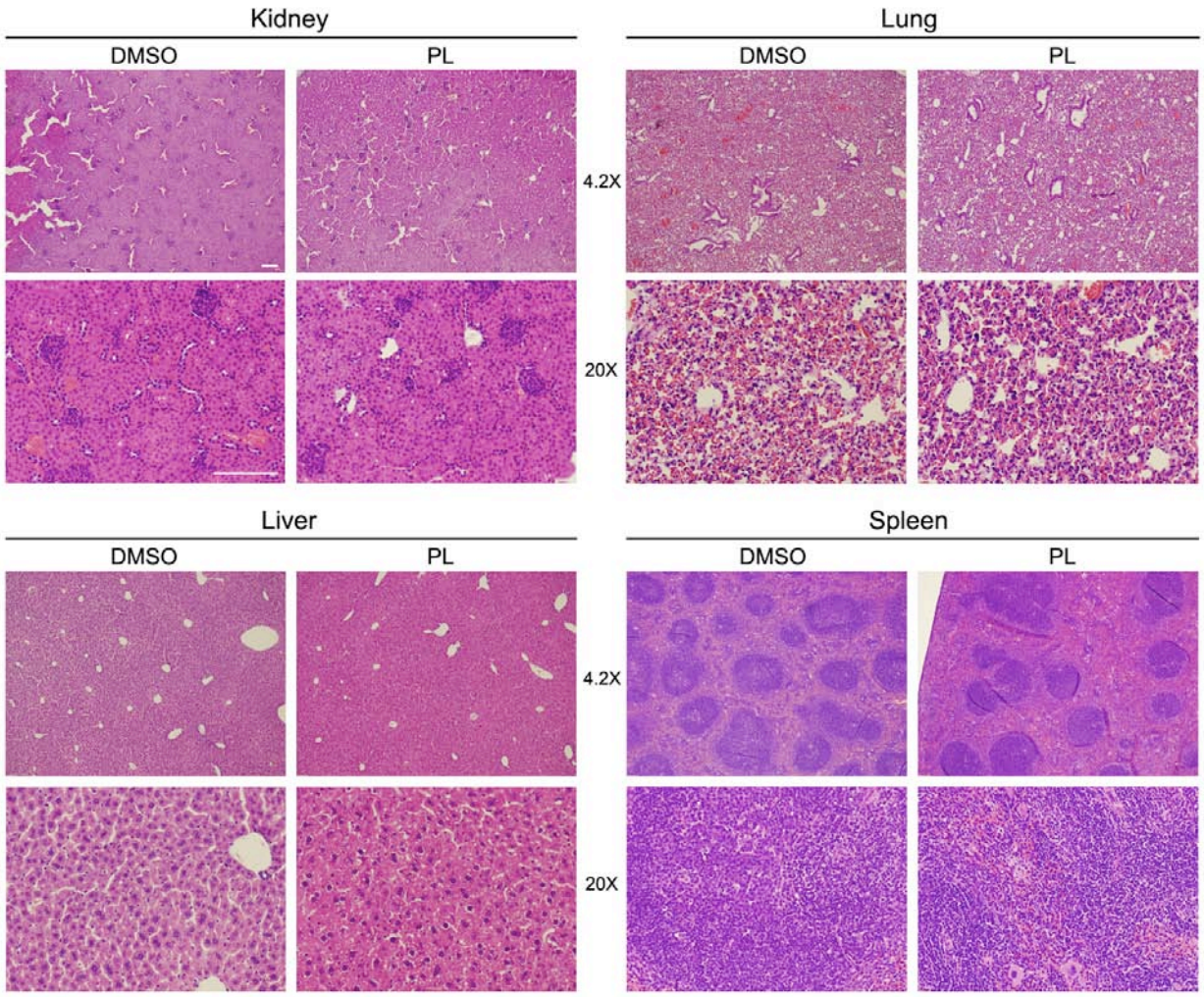

Supplemental Figure 13. Histological morphology of hematoxylin-eosin stained tissue sections from several organs (kidney, liver, lung and spleen) of CD mice treated with PL or DMSO daily for 6 days (from Suppl. Fig. 11). CD mice were administered with PL at 2.4 mg/kg intraperitoneally for daily for 6 days. After collecting blood samples for hematology, the animals were sacrificed, and the vital organs were collected for histo-pathological analysis, and analyzed by Dana-Farber/Harvard Cancer Center (rodent histopathology core) pathology services. The organs (kidney, liver, lung and spleen) were fixed in formalin over-night and processed for a paraffin embedding. The paraffin embedded block

were sectioned and stained by hematoxylin and eosin. The slides were photographed using a 4.2X and 20X objective. Scale bar, 100 μM. Histopathological evaluation of the Hematoxylin/Eosin stained slides of the vital organs by an experienced pathologist (Dana-Farber/Harvard Cancer Center, rodent histopathology core) did not reveal any significant difference between the control and PL treated groups.

a **Rat** (Sprague Dawley)

Group	Dosing route	Dosage (mg/kg)	Animal Number	Animal Death during Study Days		Total Animal Death (%)
				Within 6hrs	6-24hrs	
			♂	♂	♂	♂
1	PO	100	3	0	0	0
2	PO	300	3	0	0	0
3	PO	1000	3	0	0	0
4	PO	2000	3	1	0	33.3

b **Mice** (CD-1)

Group	Dosing route	Dosage (mg/kg)	Animal Number	Animal Death during Study Days		Total Animal Death (%)
				Within 6hrs	6-24hrs	
			♂	♂	♂	♂
1	PO	100	3	0	0	0
2	PO	300	3	0	0	0
3	PO	1000	3	0	0	0
4	PO	2000	3	0	1	33.3

Supplementary Figure 14. Clinical observations of the toxicity studies of PL in rat (a) and mice (b). (a) Summary of animal death in SD rats following single oral administration. The objective of this study is to determine the toxicity of PL in SD rats following single oral administration at 100, 300, 1000 and 2000 mg/kg. For this purpose, twelve male SD rats were divided into four dosage groups, each with three rats. The test article PL was dissolved in 20% PEG400/0.25% Tween-80/79.75% water for oral administration. **(b)** Summary of animal death in CD-1 mice following single oral administration. The objective of this study is to determine the toxicity of PL in CD-1 mice following single oral administration at 100, 300, 1000, and 2000 mg/kg. For this purpose, fifteen male CD-1 mice were divided into four dosage groups, each with six mice. The test article PL was dissolved in 20% PEG400/0.25% Tween-80/79.75% water for oral administration.

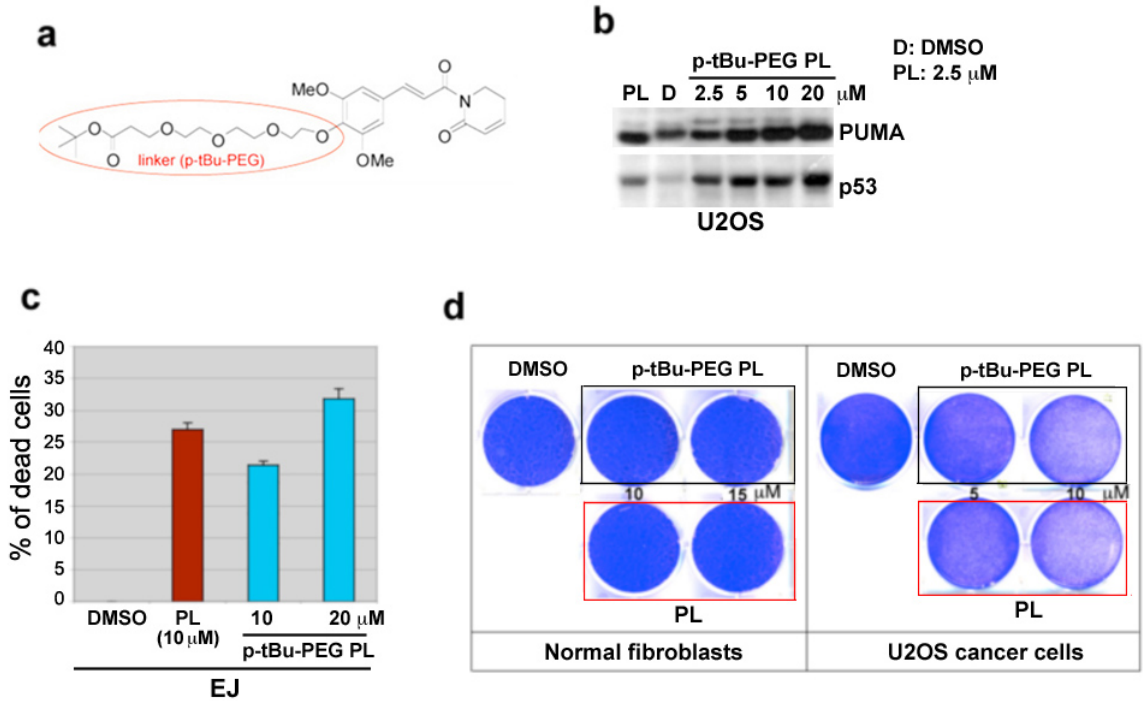

Supplementary Figure 15. P-tBu-PEG PL: a PL analog for target identification. (a) Structure of a PL analog with a linker used for PL target identification. The affinity reagent was prepared by attaching the linker to PL, which does not affect cellular activity of PL, and by tethering the linker-attached PL to a solid support. **(b)** P-tBu-PEG PL activates p53 and its proapoptotic target PUMA. U2OS cells were treated with PL (2.5 μM), various concentrations of a PL analog P-tBu-PEG PL (2.5-20 μM), or DMSO (D) for 12 hours, and western blotting was performed to measure expression of p53 and PUMA. **(c)** P-tBu-PEG PL induces cell death in EJ cancer cells containing dysfunctional p53 as similar to that of PL treatment. Cytotoxicity was measured by trypan blue exclusion staining cell viability assay after 12 hr of PL treatment, and representative graph is shown (mean ± SD of three independent experiments). **(d)** P-tBu-PEG PL also selectively induces cell death in U2OS cancer cells. Normal human skin

fibroblasts and U2OS cancer cells were treated with PL and P-tBu-PEG PL, respectively, for 12 hour, and cell viability was assessed by crystal violet staining.

a

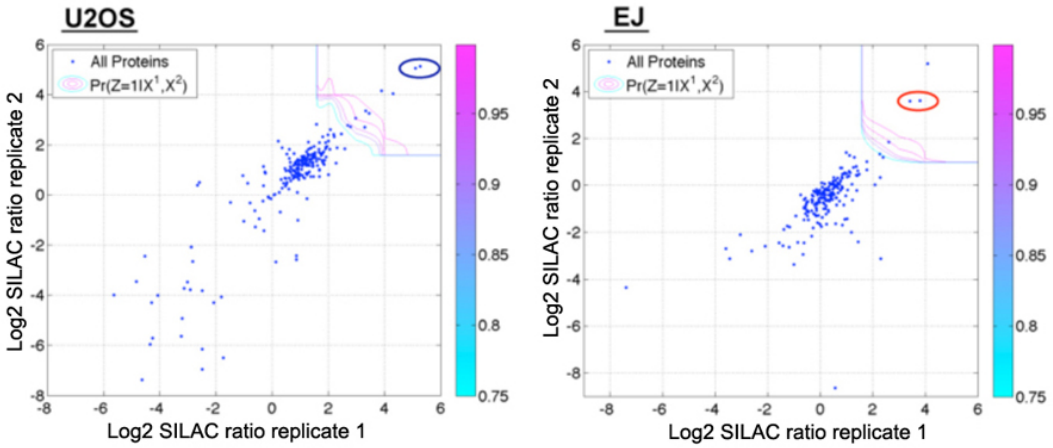

b

	Targets identified by SILAC	U2OS (wt-p53) soluble competitor 10.7X	U2OS (wt-p53) soluble competitor 107X	EJ (mutant p53) soluble competitor 14.3X	EJ (mutant p53) soluble competitor 71.5X	combined local fdr
→	**GSTpi**	7.64E-17	3.22E-24	3.87E-23	1.01E-09	3.114E-23
→	**CBR1**	4.94E-18	1.51E-29	1.41E-16	8.29E-09	2.007E-22
→	GSTZ1	4.52E-09	7.41E-13		1.85E-17	1.512E-10
→	GSTM3	3.02E-08	1.05E-14			5.097E-07
	AHNAK	0.568047				4.504E-05
	PLEKHM1	5.41E-13	1.01E-11			4.881E-05
→	GLO1	0.008171		0.014064	0.00959	0.0097037
→	GSTO1	0.000291	0.065458		0.05865	0.0175819
	ANXA5	0.000302	0.009648	1	1	0.0966072
	RPS5	0.942564	0.856822	0.063225	0.64276	0.0966415
	VIM	1	1	0.050217	0.768993	0.0967923
→	PRDX1	1	1.3E-05	0.847564	0.83629	0.1200278

Supplementary Figure 16. Identification of PL-targets via SILAC and quantitative proteomics. EJ (mutant p53) and U2OS (wt-p53) cells were cultured in medium containing either the 'light', natural isotope abundance forms, or the 'heavy' ^{13}C, ^{15}N-bearing versions of arginine and lysine. **(a)** Identifying significant targets of PL in soluble competition data. Scatter plots of 2 replicate

experiments of PL using 107 fold excess of PL (over the amount loaded on beads) as soluble competitor. Panel A; U2OS cell line, Panel B; EJ cell line. Each data point is a single protein. The contour lines demarcate a local FDR of 0.001, 0.01, 0.05, 0.1, 0.75 from outermost to innermost, and all data points to the top right corner of the plot are inferred targets. Circled in red and blue are GSTP1 and CBR1 in EJ and U2OS cells respectively, the targets with the lowest combined FDR for all experiments.

(b) Identification of target proteins specifically bound to PL in EJ and U2OS cells. Specific PL-protein interactions were identified by SILAC methodology**.** Cancer cell populations were fully labeled with light and heavy amino acids, and lysates were incubated either with PL-loaded beads (PL-Beads) in the presence of soluble PL competitor or PL-Beads alone. Proteins interacting directly with soluble PL were enriched in the heavy state over the light and identified with differential ratios. Non-specific interactions of proteins were enriched equally in both states and had ratios close to one. The individual false positive probabilities are indicated in each experiment (consisting of two technical replicates each), where an absent value indicates that the protein was not identified in that experiment. Target molecules are ranked according to the lowest combined false positive probability (last column on the right). Red arrows indicate proteins involved in the regulation of cellular response to oxidative stress.

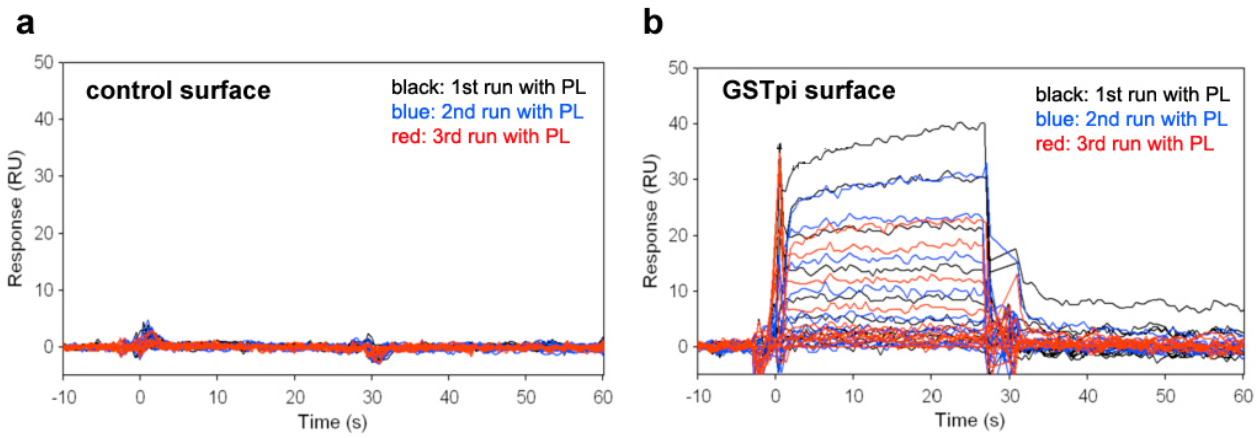

Supplementary Figure 17. The binding of PL to biologically active GSTpi was measured using BiAcore approach. PL was tested in a 1.5-fold dilution series starting at 300 μM. The entire concentration series was tested three times. **(a)** No binding was detected on the control surface. **(b)** PL binds in a concentration-dependent manner to the GSTpi surface. The decrease in signal over the three runs suggests the recombinant GSTpi is losing activity during the analysis.

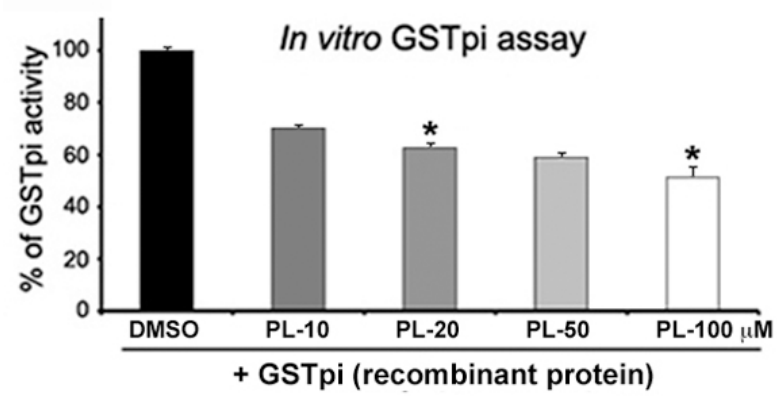

Supplementary Figure 18. GSTpi enzyme activity was measured with/without PL treatment *in vitro*. In the assay for *in vitro* measurement of GSTpi enzymatic activity, recombinant GSTpi protein (PROSPEC, Inc.) was used in a final reaction volume of 200 µl that contained 100 mM potassium phosphate buffer (pH 6.5), 1 mM EDTA (pH 6.5), 0.25 mM glutathione and 0.2 mM ethacrynic acid. The amount of ethacrynate-GSH conjugates was measured by spectrophotometry at 270 nm. The GSTpi enzymatic activity of the DMSO treated sample was arbitrarily was defined as 100% and the change in GSTpi activity in PL treated samples were plotted accordingly. Error bars represent mean $\pm$ SD of four experiments; *$p<0.0001$. The GSTpi-specific activity was measured by using ethacrynic acid, a GSTpi class–specific substrate.

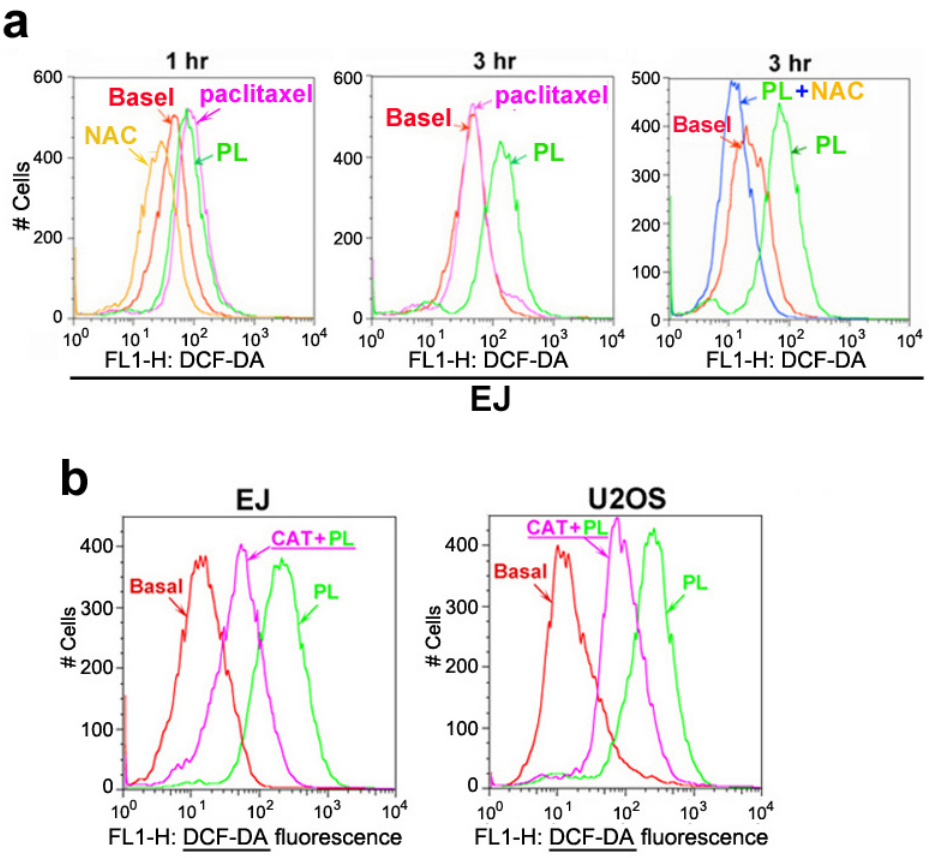

Supplementary Figure 19. PL-induced ROS elevation and reversion by NAC and catalase in cancer cells were measured by flow cytometry using DCF-DA. (a) EJ cells were treated with PL (10 μM), paclitaxel (25 nM), NAC (3 mM), or DMSO (basal) for 1 h and 3 h, and also pretreated with 3 mM NAC for 1 h, followed by 10 μM PL for 3 h. ROS were then measured by flow cytometry using DCF-DA and comparisons of ROS in EJ cells induced by PL and paclitaxel were shown by histograms. **(b)** Reversion of PL-induced ROS accumulation by catalase. EJ or U2OS cells were pretreated with catalase (CAT, 2,000U/ml) for 2 hr, followed by 10 μM PL for 3 h. ROS were then measured by flow cytometry using DCF-DA, and comparisons of ROS induced by PL with or without CAT were shown by histograms.

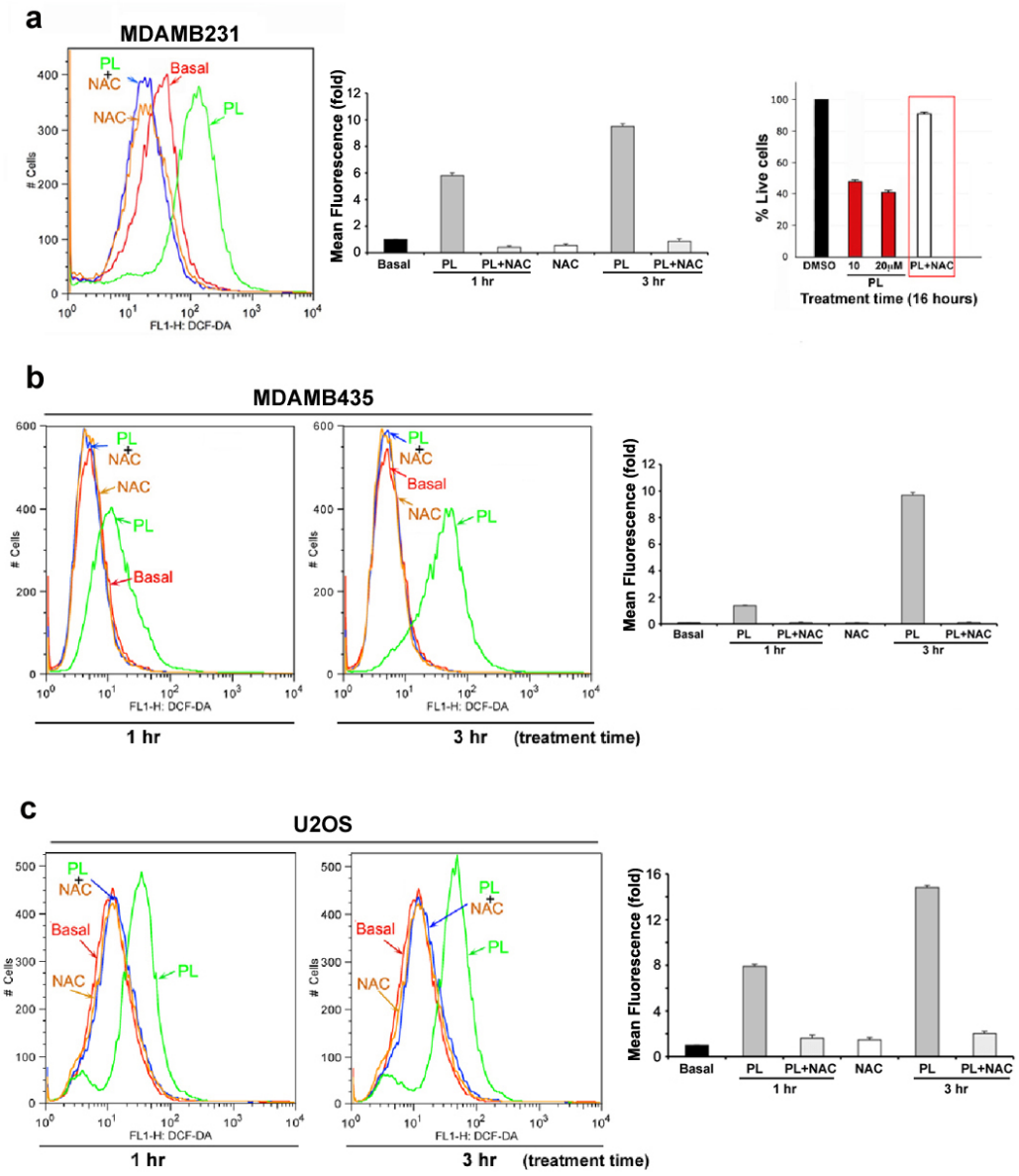

Supplementary Figure 20. PL enhances ROS accumulation in human cancer cells. (a) Induction of ROS by PL in MDAMB231 cells. PL-induced ROS and cell death can be rescued by an antioxidant NAC. MDAMB231 human breast cancer cells were treated with PL (10 μM) or DMSO (Basal) for 1 hr and 3 hr, and ROS was then measured by flow cytometry using DCF-DA. Cells were also pretreated with NAC (3 mM) for 1 hr, followed by 10 μM PL for 1 hr or 3 hr. Cell

viability was measured by Cell-Titer-Fluor cell viability assay; a representative graph is shown (mean ± SD of three independent experiments). PL-mediated ROS elevation and reversion by NAC in MDAMB231cells **(a)** MDAMB435 cells **(b)** and in U2OS cells **(c)**.

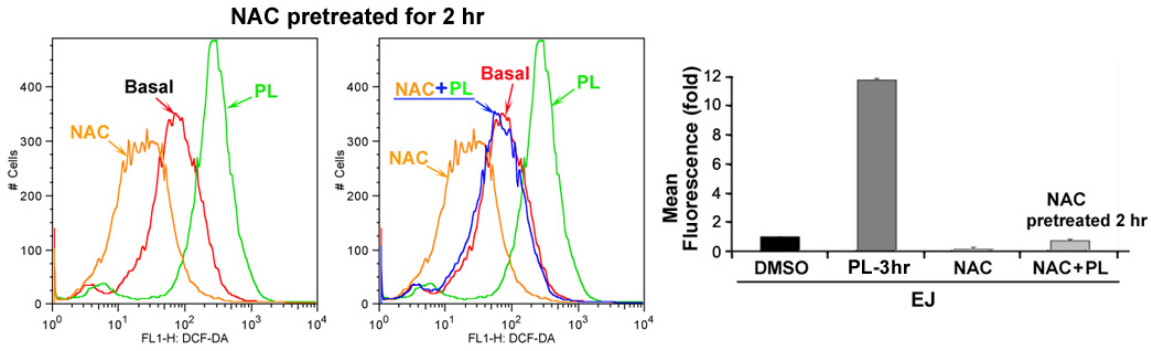

Supplementary Figure 21. Effects of antioxidant NAC on PL-induced ROS levels in EJ tumor cells. EJ tumor cells were treated with NAC (3 mM) for 2 hours, after which the cells were washed with PBS, treated with PL (10 μM) for 3 hour. ROS levels were detected by DCF-DA and fold of ROS levels calculated based on three independent experiments. Pretreatment with NAC almost completely reversed PL induced ROS accumulation. NAC is a nucleophile that can form covalent bonds with electrophilic species and a free radical scavenger.

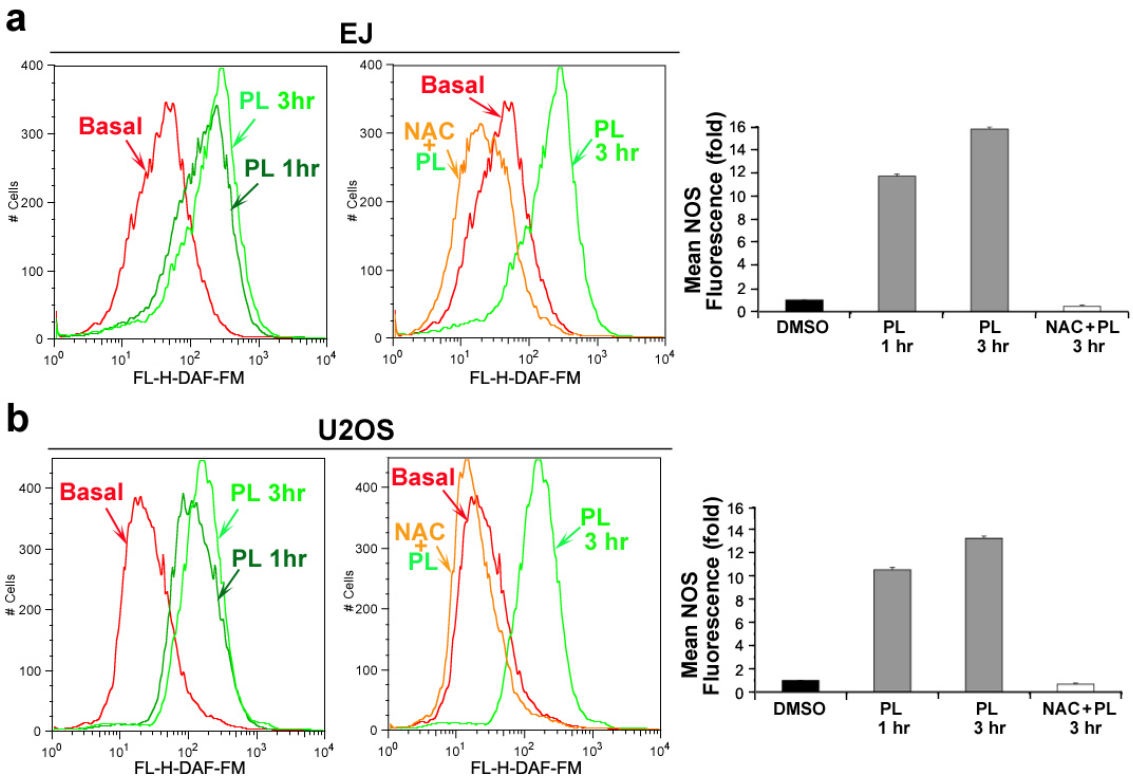

Supplementary Figure 22. PL-mediated induction of nitric oxide (NO) and its reversion by NAC. EJ and U2OS cells were pre-incubated with NAC (3mM) for 1 hr, followed by PL (10 μM) treatment for 3 hr. Nitric oxide was measured by flow cytometry after cells were labeled with 4-amino-5-methylamino-2',7'-difluorofluorescein (DAF-FM) diacetate (3 μM) for 1 hr.

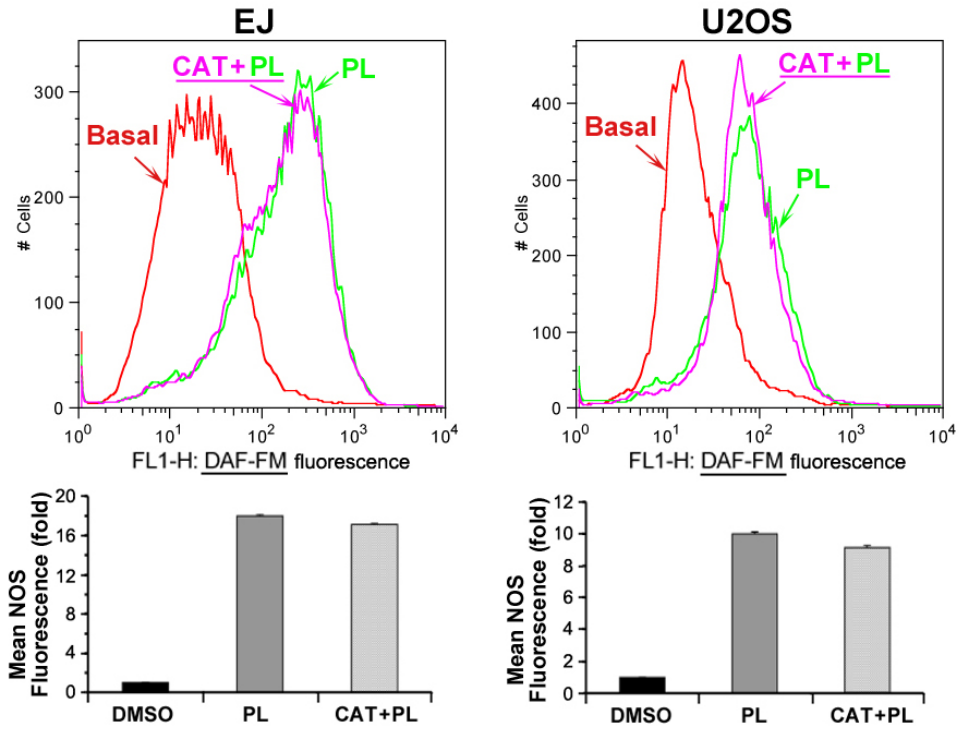

Supplementary Figure 23. PL-induced NO increase is not reversed by catalase. EJ and U2OS cells were pre-incubated with catalase (2000U/ml) for 2 hr, followed by PL (10 μM) treatment for 3 hr. Nitric oxide was measured by flow cytometry after cells were labeled with 4-amino-5-methylamino-2',7'-difluorofluorescein (DAF-FM) diacetate (3 μM) for 1 hr.

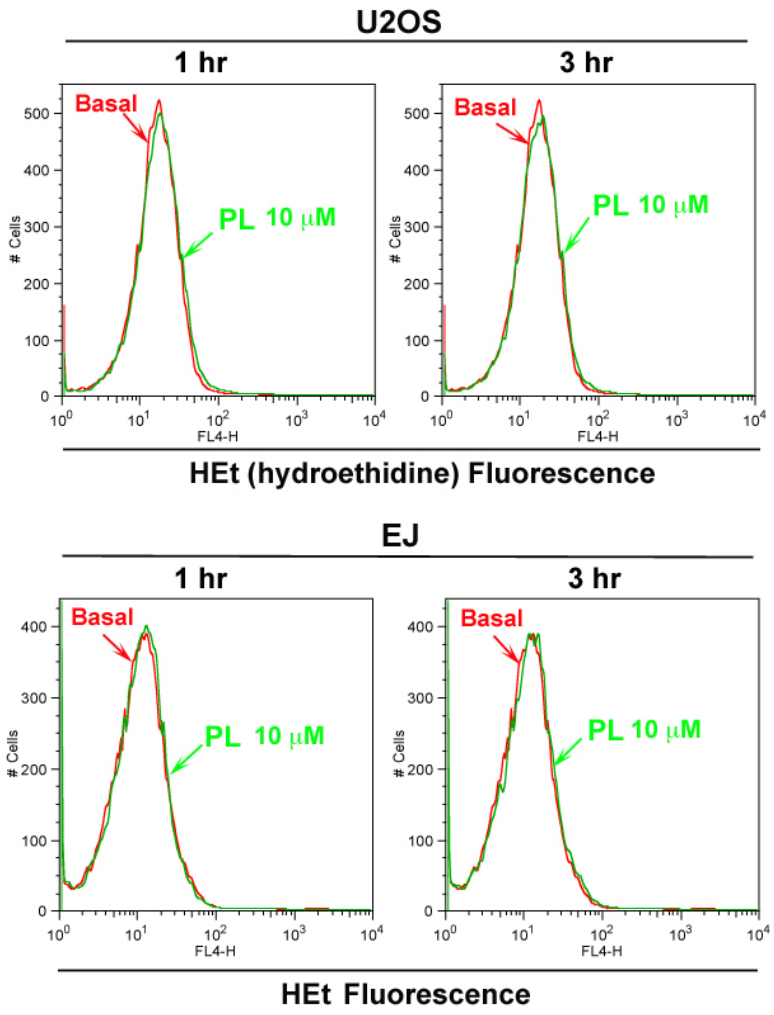

Supplementary Figure 24. Effect of PL on superoxide anion. PL did not cause any significant change of cellular superoxide levels in U2OS and EJ cancer cells. Cells were treated with PL for 1 hr and 3 hr. Cellular superoxide was measured by flow cytometry after cells were labeled with 100 ng/ml of hydroethidine (HEt) for 1 hr.

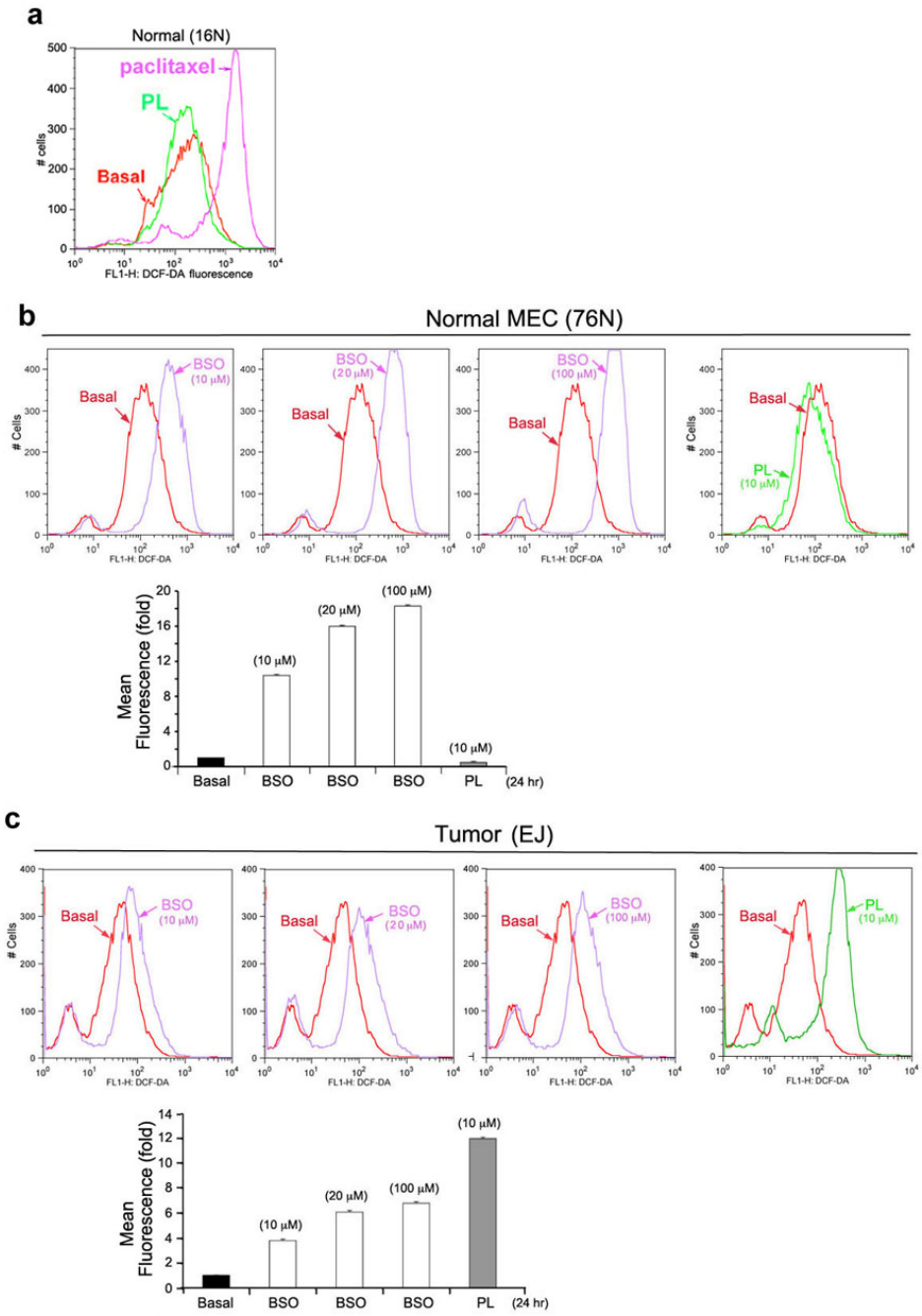

Supplementary Figure 25. BSO induced ROS accumulation in normal and cancer cells. (a) PL does not increase ROS in normal primary mammary epithelial cells (16N). 16N grown in p100mm dish were treated with PL (10 μM), paclitaxel (25 nM), or DMSO (1% V/V, Basal). ROS were measured by flow cytometry using DCF-DA. **(b)** Normal mammary epithelial cells (76N) and **(c)** tumor cells (EJ) were treated

with increasing concentrations of BSO (10-100 μM) and 10μM of PL for 24 hours. 76N as well as all other normal cells used in the entire study were grown in respective “primary cell” growth media; subjected to experimental conditions in 100mm or 6-well tissue culture plates, before passage 5 and always at ~ 80% confluency. ROS accumulation was detected by DCF-DA flow cytometry. BSO, a known inhibitor of glutathione synthesis, elevated ROS levels in both normal and tumor cells in a dose-dependent manner. In comparison, PL induced ROS levels only in tumor cells. This result is consistent with our previous observation that demonstrates that PL selectively induces ROS levels in oncogenically transformed cells and not normal cells.

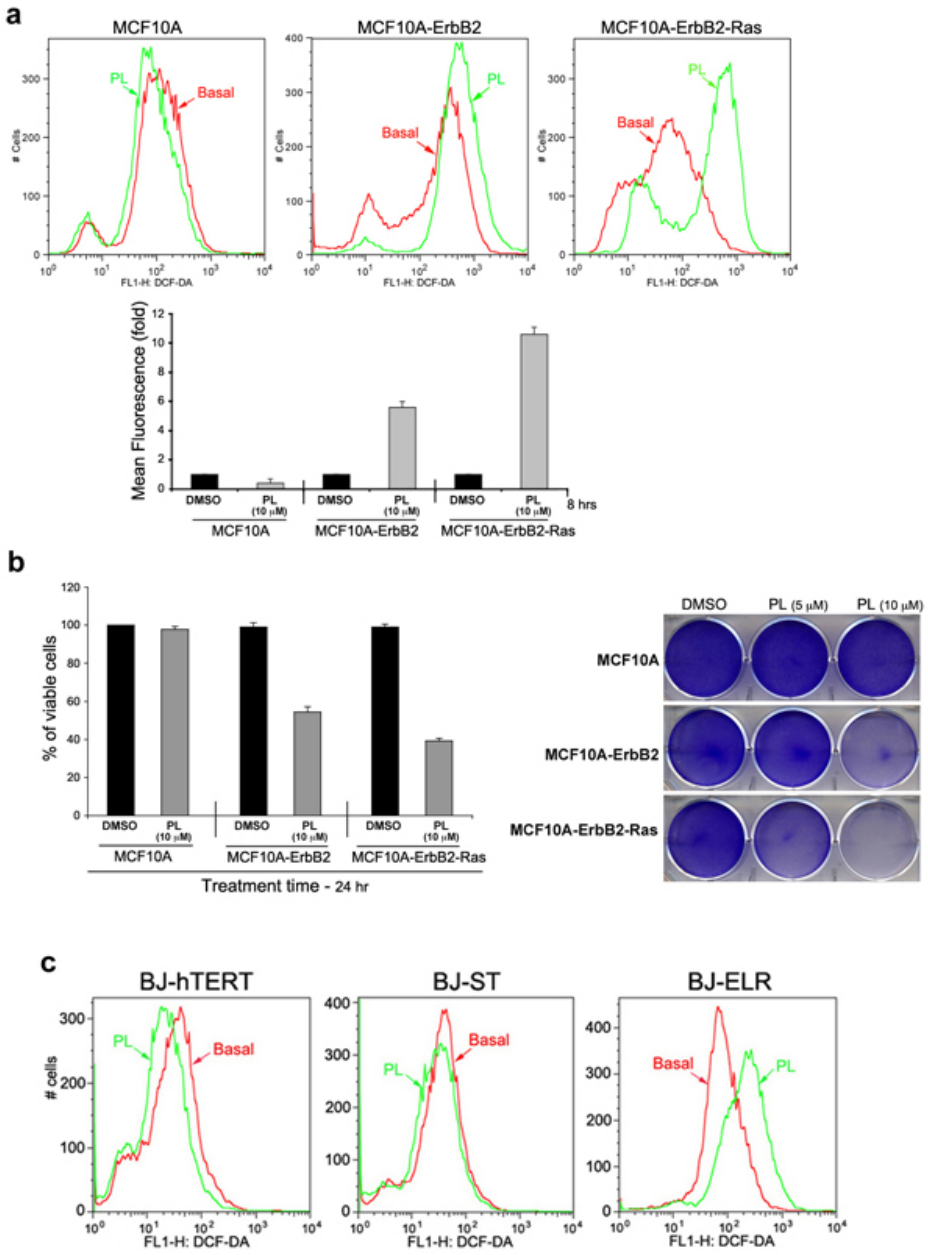

Supplementary Figure 26. PL induces ROS and cell death selectively in oncogenically transformed cells. (a) Immortalized mammary epithelial cell line MCF10A and a sub-line MCF10A-ErbB2-Ras (transformed with ErbB2 and the oncogenic H-Ras) were subjected to PL for 8 hours. Increase in ROS levels were observed only in MCF10A-ErbB2-Ras and not the parental MCF10A cell-line. **(b)** PL treatment for 24 hours did not affect the viability of MCF10A cell-line, but

significantly decreased the viability of MCF10A-ErbB2-Ras cells as plotted graphically. Cell viability was measured by trypan blue exclusion assay; a representative graph is shown (mean ± SD of three independent experiments). The right panel shows cell survival by crystal violet staining assay. **(c)** Selective induction of ROS by PL in oncogenically transformed BJ human fibroblasts (BJ-ELR) but not in non-transformed BJ fibroblasts (BJ-hTERT and BJ-ST). The ROS levels of human BJ skin fibroblasts immortalized by the expression of the catalytic subunit of human telomerase (BJ-hTERT) and SV40 large T antigen (BJ-ST) or transformed by Ras oncogene (BJ-ELR) were measured by DCF-DA flow cytometry after treating with PL (5 μM) for 8 h.

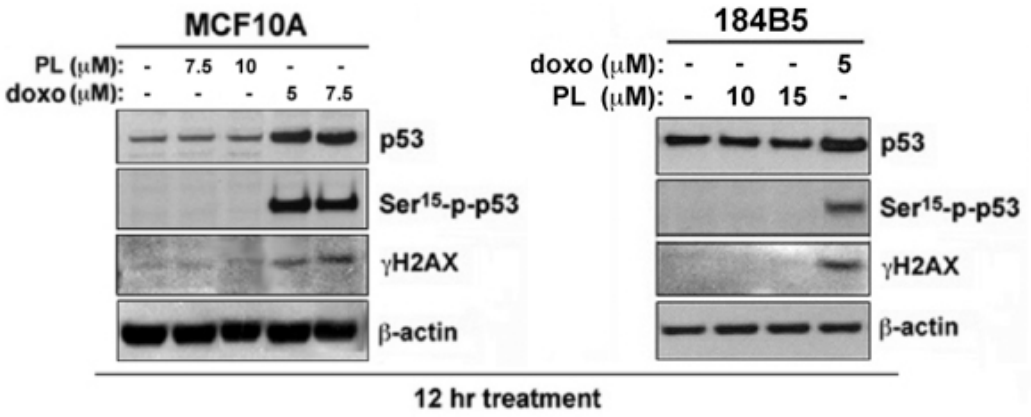

Supplementary Figure 27. PL does not induce the expression of DNA damage response targets in immortalized cells. The effect of PL on stress response targets was determined by western blot analysis of p53, Ser15-phospho-p53, and γ-H2AX in PL (7.5 and 10 μM) treated immortalized human breast epithelial cells (MCF10A & 184B5). Cells were treated with PL, doxorubicin (doxo, 5 and 7.5 μM), or DMSO as solvent control for 12 hrs. β-actin expression was used as a loading control. Note that expression of p53, phospho-p53, and γ-H2AX was induced in response to DNA-damaging agents, doxo but not with PL in normal cells.

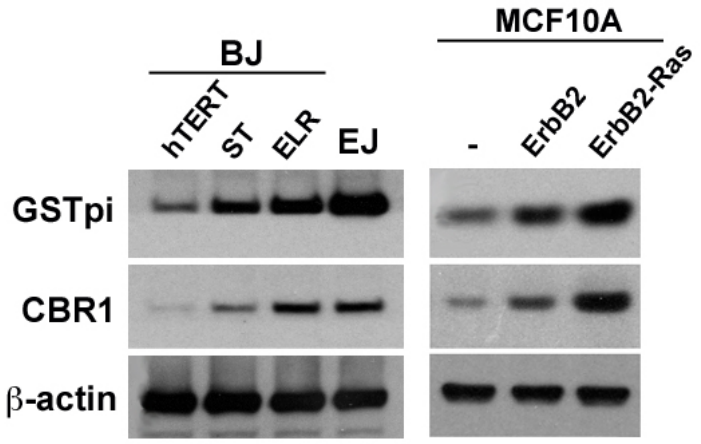

Supplementary Figure 28. The expression of GSTpi and CBR1 is enhanced in oncogenically transformed cells and human cancer cells. Basal expression levels of GSTpi and CBR1 were determined by western blot analysis in non-transformed (BJ-hTERT, BJ-ST) and oncogenically transformed BJ fibroblasts (BJ-ELR) as well as EJ cancer cells. Expression levels of GSTpi and CBR1 were also determined by western blot analysis in MCF10A and sublines MCF10A-ErbB2 and MCF10A-ErbB2-Ras.

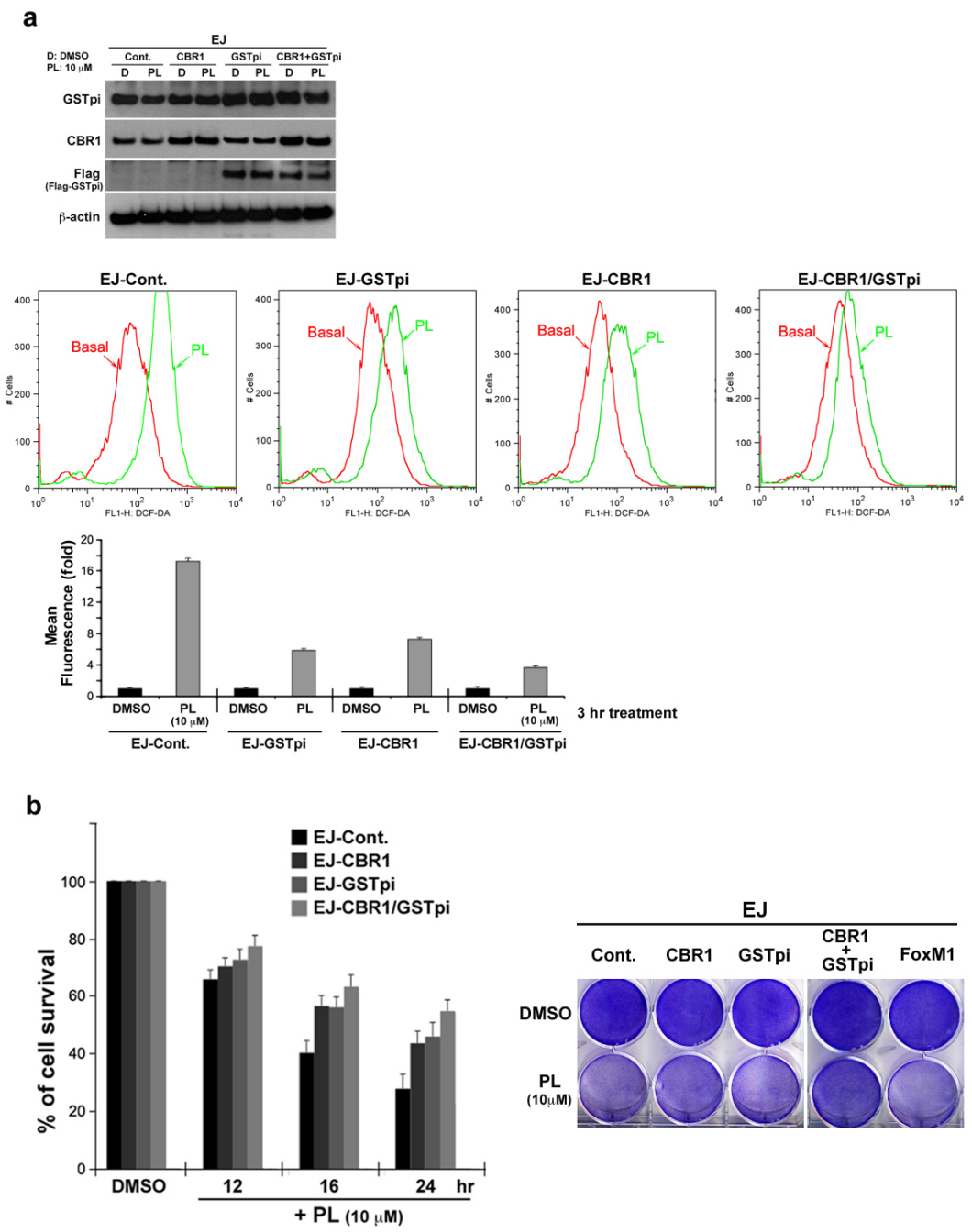

Supplementary Figure 29. Exogenous expression of GSTpi and CBR1 ameliorates PL-induced ROS and cell death. (a) Overexpression of GSTpi and CBR1 reduces the PL-mediated ROS increase in EJ cancer cells. EJ cells were transfected with empty vector (pcDNA3.1), CBR1, GSTpi (Flag-GSTpi), or both CBR1 and Flag-GSTpi. The pool of stable clones expressing these constructs

was treated with DMSO (0 h) or 10 μM PL for indicated time points. ROS was measured by flow cytometry using DCF-DA. ROS levels were also shown by histograms and quantitative bar graph (the low panel). **(b)** PL-induced cell death can be rescued by overexpression of both GSTpi and CBR1. EJ cells stably expressing GSTpi, CBR1, or both were treated with PL for indicated times. Cell viability was then assessed using trypan blue exclusion; a representative graph is shown (mean ± SD of three independent experiments). The right panel shows cell viability staining using crystal violet after PL treatment for 16 hours. EJ cells overexpressing FoxM1 was also used for cytotoxic assay as an overexpression control.

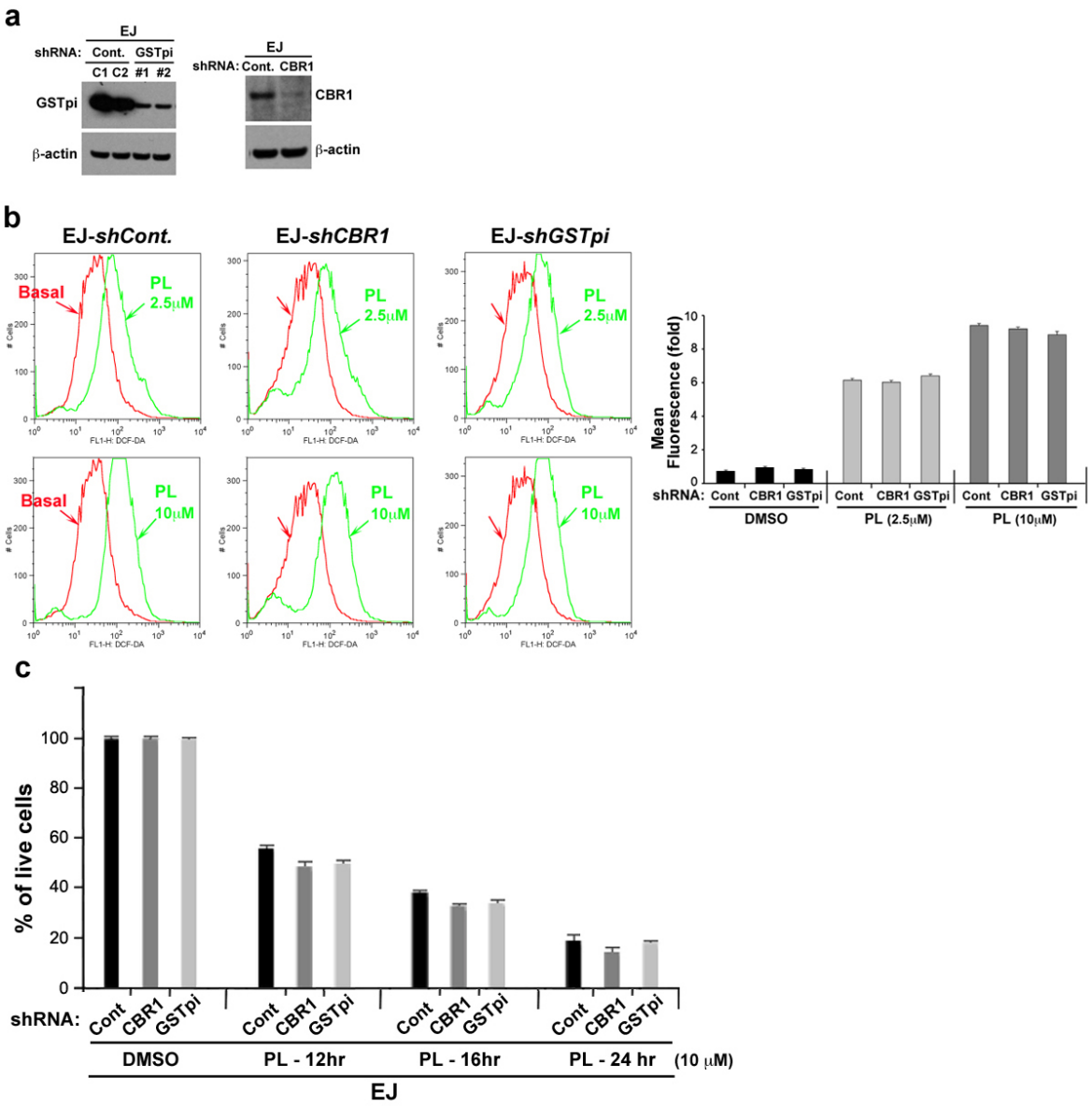

Supplementary Figure 30. Knockdown of GSTpi or CBR1 does not affect PL-mediated ROS increase and cell death. Knockdown of *GSTpi* and *CBR1* in EJ cells does not significantly alter the ROS levels induced by PL when compared to the parental EJ cells. EJ cells with stably transfected shRNA directed against *GSTpi* and *CBR1* were generated to establish EJ-*GSTpi* knockdown (EJ- *GSTpi* KD) and EJ-*CBR1* knockdown (EJ- *CBR1* KD) lines. **(a)** The knockdown was confirmed by western blotting using anti-CBR1 and anti-

GSTpi antibodies. **(b)** PL-mediated ROS levels were measured by DCF-DA in these sub-lines and compared to the parental EJ cell-line. Comparison of ROS levels between the sub-lines and parental EJ cell-line did not show a significant difference at two different PL concentrations (2.5 μM and 10 μM). **(c)** Cell viability was measure by trypan blue exclusion assay.

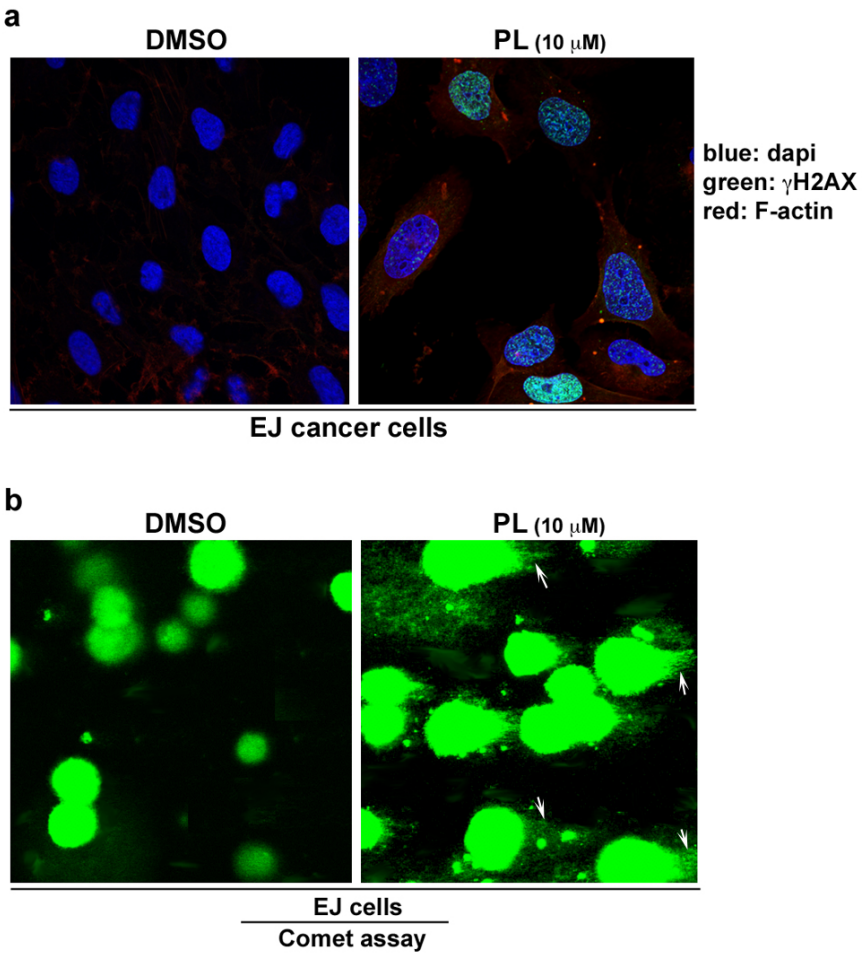

Supplementary Figure 31. PL-induced DNA damage in EJ tumor cells. (a) PL treatment increases an expression of a DNA damage marker γH2AX. EJ cells were incubated with 10 μM PL or DMSO for 12 hours. Cells were then subjected to immunofluorescence staining using antibodies against γH2AX and F-actin (control) and counterstained by dapi. **(b)** Comet tail formation in PL-treated EJ cells. In response to PL, EJ cells have accumulated damaged DNA that migrated out of the cell (arrows).

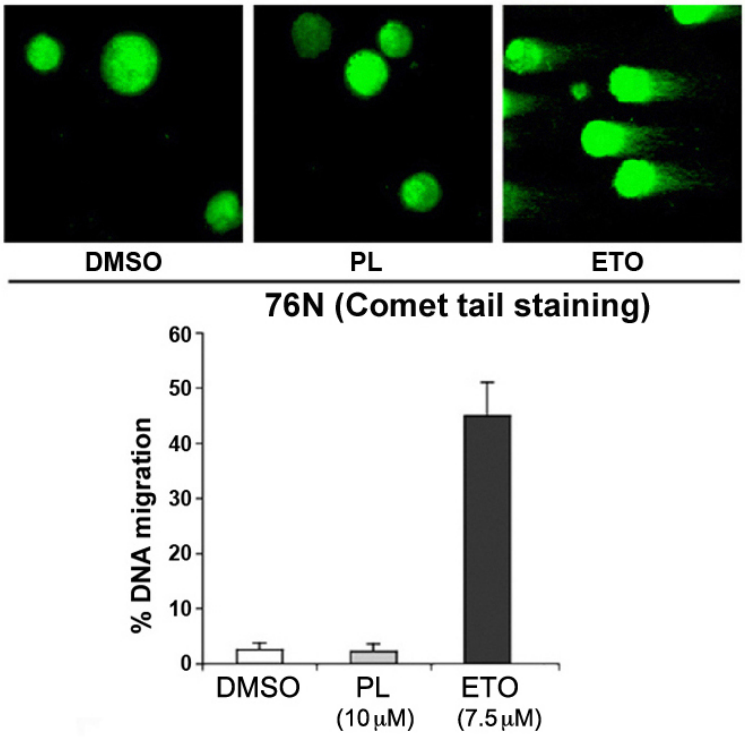

Supplementary Figure 32. No comet tail formation in PL-treated 76N normal cells. 76N cells were treated with etoposide (ETO, 7.5 μM), solvent (DMSO), and PL (15 μM) for 12 h. After treatment, cells were embedded into an agarose gel and the proteins and lipids were removed by exposing the gel to an alkaline NaOH solution. DNA fragments were separated from the nucleus (comet head) by gel electrophoresis and visualized by staining with SYBR-green I using confocal microscopy. In DMSO and PL treated cells (under electrophoresis) the SYBR Green I fluorescence is confined to the nuclei. In response to ETO, cells have accumulated damaged DNA that migrated out of the cell and could be qualitatively scored according to the intensity of comet tail formed. For determining the comet tail intensity at least 80 cells per sample were scored using a 63X objective on a Leica TCS-NT confocal microscope. Each panel represents three random fields per sample captured by the confocal microscope.

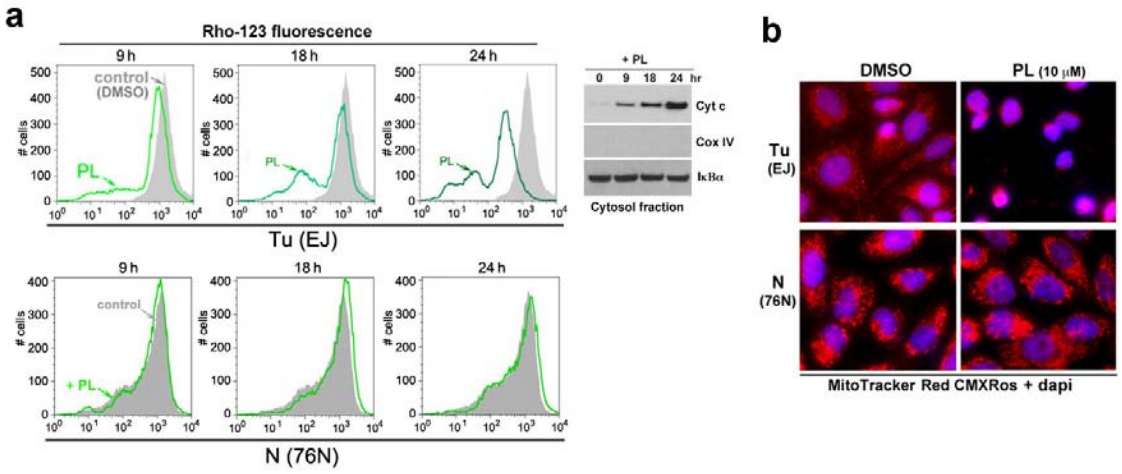

Supplementary Figure 33. PL-induced decrease of mitochondrial membrane integrity/potential in cancer cells. (a) EJ cells were incubated with 10 μM PL or DMSO (control solvent) for 9, 18, and 24 h, respectively. The integrity of mitochondrial membranes was measured using rhodamine-123. The release of cytochrome c to cytosol in EJ cells treated with PL was also determined by western blot analysis using cytosol fraction extracts. Fractionated cytosol lysates were assessed for the presence of cytochrome c, Cox IV (mitochondrial fraction), and IκBα (cytosolic fraction). **(b)** Mitochondrial morphology was assessed by MitoTracker ®Red CMXRos stain, and nuclei were counterstained by dapi. PL-treated EJ and 76N cells (10 μM for 24 hours), respectively, were treated visualized by fluorescence microscopy. Noted that EJ cells after PL treatment showed condensed clumping of the mitochondria.

1 Brown, L. *et al.* CDIP, a novel pro-apoptotic gene, regulates TNFalpha-mediated apoptosis in a p53-dependent manner. *The EMBO journal* **26**, 3410-3422 (2007).
2 Stegmaier, K. *et al.* Signature-based small molecule screening identifies cytosine arabinoside as an EWS/FLI modulator in Ewing sarcoma. *PLoS Med* **4**, e122, doi:06-PLME-RA-0677R2 [pii] 10.1371/journal.pmed.0040122 (2007).
3 Lamb, J. *et al.* The Connectivity Map: using gene-expression signatures to connect small molecules, genes, and disease. *Science (New York, N.Y* **313**, 1929-1935, doi:313/5795/1929 [pii] 10.1126/science.1132939 (2006).